Bulletin of the Earthquake
Research Institute
Vol. 40 (1962), pp. 431-493

21. *Some Investigations on the Character of Crustal Deformation.*

By Atusi Okada,

Earthquake Research Institute.

(Read June 27 and Oct. 24, 1961.—Received June 30, 1962.)

Contents

Introduction 431
Chapter 1. Classification of Vertical Crustal Deformation 434
§ 1. Sudden Crustal Deformation Accompanied by Seismic Activities 434
§ 2. Secular Crustal Deformation 437
Chapter 2. Relation between Shallow Earthquake and Upheaval 443
§ 1. Distribution of Displacement Accompanied by Shallow Earthquakes in the Area of Upheaval 443
§ 2. Relation between Vertical Displacement and Depth of Hypocenter 448
§ 3. Energy of Shallow Earthquakes Presumed from Analysis of Vertical Displacement 452
Chapter 3. Correlation between Secular Crustal Deformation and Gravity Anomaly 457
§ 1. Relation between Annual Mean Velocity of Depression and Gravity Anomaly along the Coast-line in South-western Japan 458
§ 2. Comparison of Crustal Deformation in Japan with that in Fennoscandia 467
§ 3. Correlation between Secular Crustal Deformation and Gravity Anomaly along the Pacific Coast-line in Japan 471
Conclusion 479
Acknowledgment 481

Introduction

The relation between seismic activity and crustal deformation, which may be brought to light with the aid of geodetic means, has been best studied in Japan[1),2)]. Crustal deformation on a large scale has been

1) C. Tsuboi, "Investigation on the Deformation of the Earth Crust Found by Precise Geodetic Means," *Jap. Jour. Astr. Geophys.*, **10** (1932), 93-213.

2) N. Miyabe, *Tikaku no Hendô* (1942), 117-202.

precisely measured on occasions of great earthquakes that occurred off the Pacific coast of the south-western part of Japan. For example, conspicuous upheavals were observed at the extremities of the Miura and Bôsô Peninsulas at the time of the Kwantô Earthquake (Sept. 1st, 1923), and also at the points of the Kii and Muroto Peninsulas at the time of the Nankaidô Earthquake (Dec. 21th, 1946)[3]. These vertical displacements were accurately detected by first order precise levelling or by mareographical observations. In south-western Japan, the epicenters of such great earthquakes are usually located far off the Pacific coast while their depths are as shallow as 30-60 km. Furthermore, these earthquakes are supposed to be accompanied by crustal deformation on the sea bottom, because violent tsunamis were experienced along the coast soon after the earthquakes. According to the statistical studies of earthquake occurrence, it has been concluded that an earthquake having a magnitude larger than 7.5 is expected to occur once every 100-200 years somewhere off the Pacific coast in this part of Japan.

Even in north-eastern Japan, the occurrence interval of great earthquakes accompanying such large tsunamis as "Sanriku tsunamis" in 1896 is about the same as that in the south-western Japan though no conspicuous crustal deformation has been observed in the Tôhoku district.

Since 1880, with the development of geodetic survey, many geophysicists conducted detailed studies on sudden crustal deformation accompanied by great earthquakes like the ones previously mentioned: the upheavals exceeding 1 meter at the points of the Miura and Bôsô Peninsulas in the case of the Kwantô Earthquake were confirmed by repeating precise levelling surveys before and after the earthquake and also by the changes in the mean sea level recorded on the mareograms at Aburatubo. The uplifts associated with earthquake occurrences at the points of the Muroto and Kii Peninsulas and at other places were also clarified by means of geodetic methods. Furthermore, they found a tendency that the secular crustal deformation at the point of each peninsula during a period between two great earthquakes took place in the direction opposite to that of the sudden deformation at the time of earthquake[4]. On the other hand, the crustal deformations accompanied by the inland destructive earthquakes have also been investigated in detail[5].

3) G. S. I., *Compilation of the 1st order precise levelling resurvey, (Ittô Suizyunten Kensoku Seika Syûroku)*, Vol. 1 (1955), 8-11.

4) A. IMAMURA, "On Crustal Deformations Preceding Earthquake," *Japa. Jour. Astr. Geophys.*, **10** (1932), 81-92.

5) For instance, Hukui, Imaiti, Nagaoka Earthquakes.

In this paper, some characteristics of these crustal deformations are investigated. In Chapter 1, crustal deformations are classified according to their features of occurrence, especially those relating to vertical displacement of bench marks for precise levels. In Chapter 2, depths of hypocenter of destructive earthquakes which occurred inland are estimated by making use of crustal deformation data from the standpoint of an elastic deformation theory. In Chapter 3 is discussed the relation between gradual crustal depression and gravity anomalies along the Pacific coast in south-western Japan. The correlation between gradual crustal deformation and Bouger gravity anomalies along the Pacific coast-line of Japan is also studied in this chapter with reference to the geographical distribution of epicenters of great earthquakes.

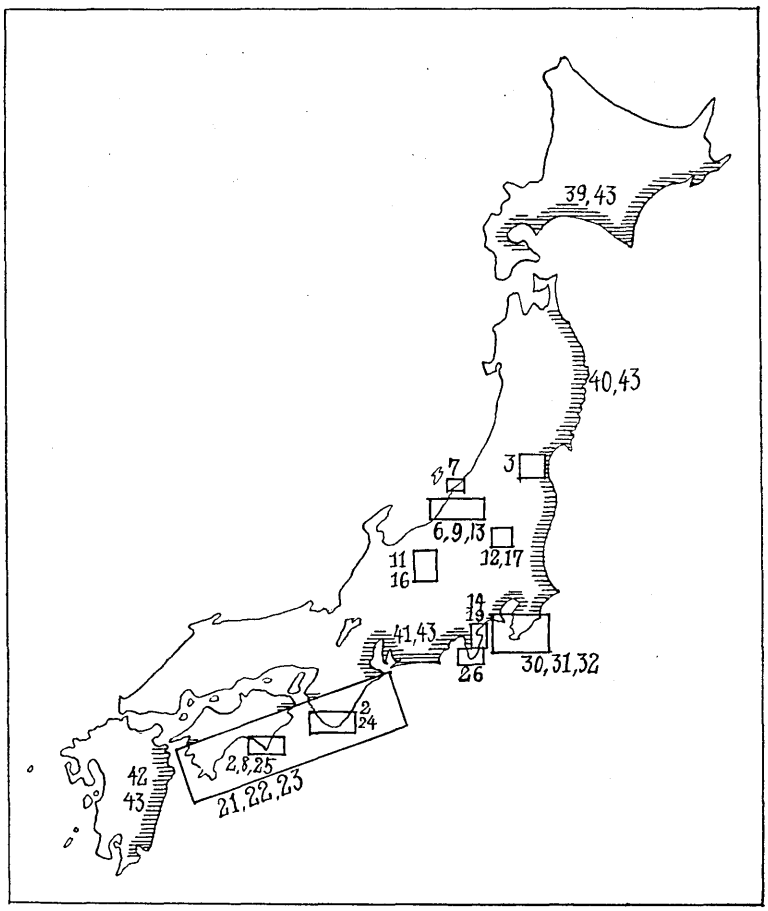

Fig. 1. Index map of Figures.

Chapter. 1. Classification of Vertical Crustal Deformation

Crustal deformations are classified as follows, on the basis of geodetic observation.

1) Sudden crustal deformation accompanied by a great earthquake.
2) Secular crustal deformation not accompanied by great earthquake.

§ 1. Sudden Crustal Deformation Accompanied by Seismic Activities

Sudden crustal deformations have often been found by geodetic precise observation after a great earthquake. These earthquakes accompanying sudden crustal deformations are generally classified as follows according to their magnitude:

(1) $8.5 \geq M \geq 7.5$, $H \leq 30$ km (M: Gutenberg-Richter's magnitude, H: Depth of the hypocenter). When these earthquakes occur off the Pacific coast of the south-western part of Japan, remarkable upheavals are observed at points of promontory in this area while there is no conspicuous crustal deformation in the Pacific coast of Hokkaidô and the north-eastern part of Japan even when great earthquakes occur off these coasts.

(2) $7.5 \geq M \geq 5.0$, $H \leq 20$ km. This kind of earthquake seems likely to cause considerable damage and crustal deformation when it occurs inland. If it occurs beneath the sea bottom, it would almost certainly give rise to tsunamis as well as crustal deformation on the sea bottom, though the tsunamis and the deformations would not be so large as those caused by earthquakes of the highest magnitude.

We classify great earthquakes occurring in and around the Islands of Japan into two groups according to their magnitude. From the point of geographic distribution, we call the first one "off Pacific side of Japan Island" and the second one "inland or Japan Sea side."

Crustal deformations are divided into three types,

1) Upheaval
2) Fault
3) Depression.

Although crustal deformation accompanying great earthquakes has often been reported in this country, not many examples of deformation were fully surveyed by geodetic methods. The Nankaidô Great Earthquake on Dec. 21th, 1946, may be regarded as one of the best examples as far as vertical crustal deformation before and after the earthquake is

concerned[6]. In this case the upheavals of the earth's surface at the Kii and Muroto points were studied so closely by a number of precise levelling surveys that even the time sequence of the tilting motion after the earthquake was brought out fairly clearly[7]. The author would here like to analyse the tilting motion at the Kii and Muroto points by making use of the results of these surveys[8),9)].

It is obviously seen in Fig. 2 that a rapid recovery of the deformation accompanied by the earthquake began immediately after the main shock, the tilt associated with the earthquake being estimated as about 6″ of arc. During 40 years or so prior to the earthquake the Kii and Muroto peninsulas had been subjected to a southerly dip. At the time of the earthquake they underwent a sudden tilting in the opposite direction, the tilting then being followed by a recovery as is already stated. If, then, we take the time origin at the moment when the main shock occurred (t is reckoned by year), the tilting angle (φ) at the Muroto point t years after the earthquake is given by an empirical formula of which the constants are determined by means of the least square method.

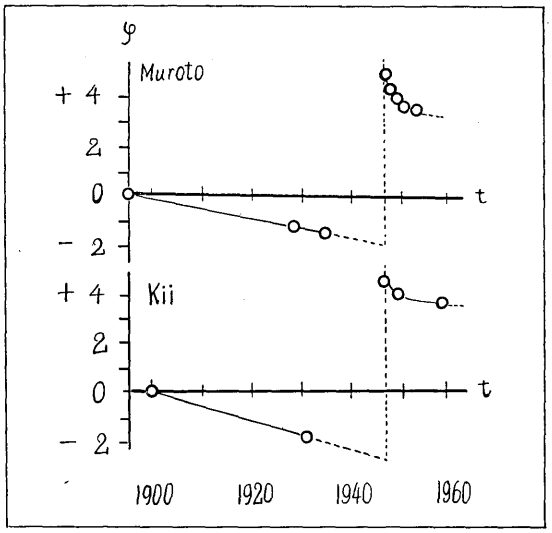

Fig. 2. Amount of tilt during 60 years at Muroto Point and Southern part of Kii Peninsula.

$$\varphi = 4.50'' + 1.65''e^{-2.232t} - 0.0348''t\,. \tag{1.1}$$

We then see that the present rate of tilting motion amounts to $-0.035''$/

6) T. NAGATA, "Summary of the geophysical investigations on the Great Earthquakes in south-western Japan on Dec. 21th, 1946," *Trans. Amer. Geophys. Union*, **31** (1950), 1-6.

7) T. NAGATA and A. OKADA, "Land deformation of Muroto Point before and after the Nankaidō Great Earthquake on Dec. 21th, 1946," *Bull. Earthq. Res. Inst.*, **25** (1948), 85-90.

8) A. OKADA and T. NAGATA, "Land deformation of the neighbourhood of Muroto Point after the Nankaidô Great Earthquake in 1946," *Bull. Earthq. Res. Inst.*, **31** (1953), 169-178.

9) A. Okada, "Land deformation of the southern part of the Kii peninsula, south-western Japan," *Bull. Earthq. Res. Inst.*, **38** (1960), 113-124.

year, while the direction of the tilt is S 10°E as has been obtained by the author.

The upheavals of each peninsula accompanied by great earthquakes, which occurred off the Pacific coast of the district, have already been pointed out through geomorphological studies on the sea shore upheaval and sea coast terrace[10]. Historical records confirm the tendency.

Faults accompanied by earthquake were investigated by many geophysicists, and some of the geophysical characteristics of earthquake faults were made clear[11].

For instance, the San Andreas Fault along the Pacific coast of the United States of America, the Neodani Fault (Nôbi Earthquake), the Gômura and Yamada Faults (Tango Earthquake), and Sikano Fault (Tottori Earthquake) were investigated in fair detail. Although in the case of the Hutatui and Hukui Earthquakes we could not find any fault on the ground surface, the hidden faults were detected clearly by means of precise geodetic levelling resurvey. We may call this kind of fault "Geodetic Fault".[12]

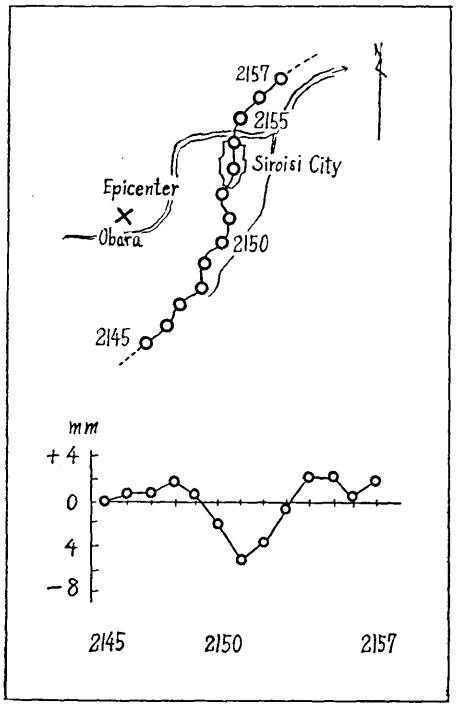

Fig. 3. Vertical displacement of bench marks near Siroisi-City.

There are few examples of depression accompanied by earthquakes. Sinking of the alluvial plane and reclaimed ground by an earthquake is simply a deformation of the ground surface which differs from essential crustal deformation. The only example of small subsidence is the Siroisi Earthquake on Sept. 30th, 1956, as shown in Fig. 3. In the case of the Siroisi Earthquake, an upheaval near the epicenter was not ascertained clearly because the changes in the

10) G. IMAMURA, *Nihon rettô no Undo.* (1944), 29-72.

11) K. KASAHARA, *Zisin no Kagaku* (1959), 96-116.

12) S. MIYAMURA and A. OKADA, Vermessung eines Teiles von Nivellierroute am Fluss Yonesiro (Dritte Mitteilung). Höhenveränderung begleitet von einen starken Lokalbeben bei Hutatui, 19, Oktober, 1955", *Bull. Earthq. Res. Inst.*, **34** (1956),373-380.

height of bench marks were measured only along the survey route 5–6 km distant from the epicenter.

In general, most depressions of the ground surface are nothing but compaction of the alluvial plane or soil deposit, excepting the above-mentioned example[13].

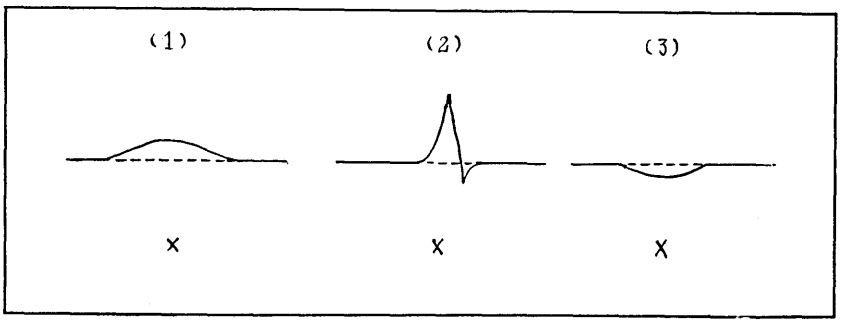

× Hypocenter

Fig. 4. Type of vertical displacement of bench marks due to sudden earth-movement.

§ 2. Secular Crustal Deformation

In the previous paragraph, the author has been concerned with sudden crustal deformation in association with earthquakes. It is also proved by geodetic study that the earth's crust often undergoes secular deformations which are continually occurring even at normal times. Since deformations of this sort are always small, they must be detected by highly accurate observations of the vertical displacement of bench marks. For this purpose, a tiltmeter may be utilized as well as levelling resurveys provided the results could be corrected for meteorological conditions, because displacements of the earth surface due to secular deformations are usually so small that they are comparable to meteorological corrections.

Secular crustal deformation is also classified into three types in a way similar to the types of sudden ones, viz.,

1) Secular upheaval
2) Activity of fault
3) Secular subsidence.

Some examples representing each of these phenomena are given in the

13) A. OKADA, "Siroisi Earthquake of Sept. 30th, 1956, and Precise Levelling Resurvey of its Epicentral Area, Miyagi Prefecture," *Bull. Earthq. Res. Inst.*, **36** (1958), 65-70.

following.

1) *Secular upheaval*

Secular upheaval movements may be classified as follows: the first is an upheaval movement in the course of attaining the isostatic equilibrium, for instance, the rising of a large area in Fennoscandia since the post-glacial age. Fig. 5 shows the relation between the uplift and geoidal undulation as obtained by the recent astrogeodetic work in the Northern European area[14].

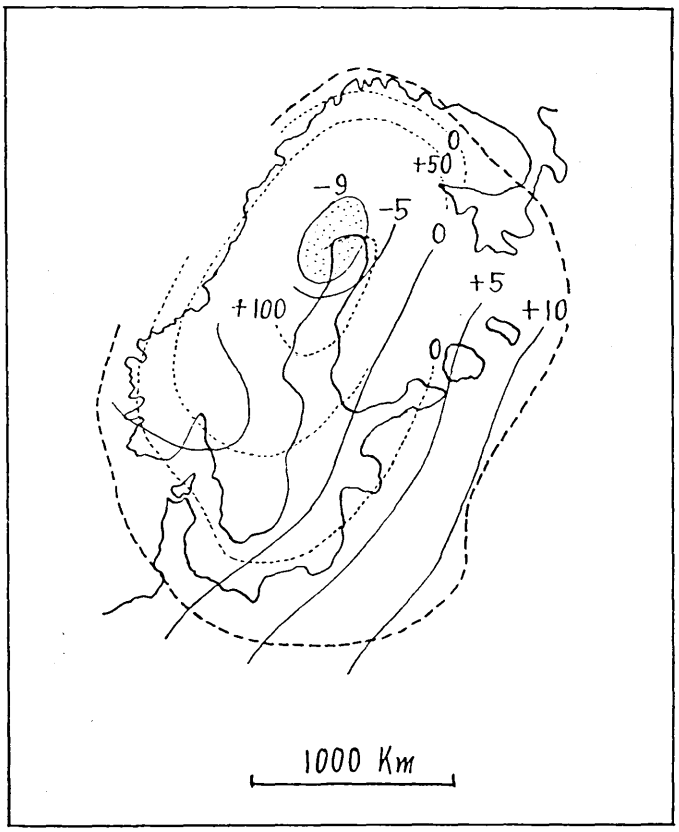

--- Recession stage of glaciation
Center of glaciation
—— Geoid contour in meter
..... Uplift during past 7000 years in meters

Fig. 5. Isoupheaval lines and geoid contour in Fennoscandia (after Irene Fischer).

14) IRENE FISCHER, "The Impact of the Ice Age on the Present Form of the Geoid," *Jour. Geophs. Res.*, **64** (1959), 85-88.

This problem will again be dealt with in Chapter 3.

In the second place, we cite an instance of active folding and warping. An active folding has already been pointed out by Prof. N. Yamazaki and Prof. Y. Ôtuka[15]. We can find some examples in the results of precise levelling resurvey over the zones of folding structure in Akita, Yamagata and Niigata districts[16]. An example in a typical oil field zone is shown in Fig. 6. The position of the maximum vertical displacement of the bench marks appears to be located at points where the route crosses the folding axes of the anticline and syncline respectively. The warpings in Tyûgoku district and Kii peninsula are also noticeable as clarified by the geodetic levelling resurvey. Recently, a warping on a small scale was found by the author when he made the precise levelling resurveys across the range of Mt. Yahiko in Niigata Prefecture[17] (as shown in Fig. 7).

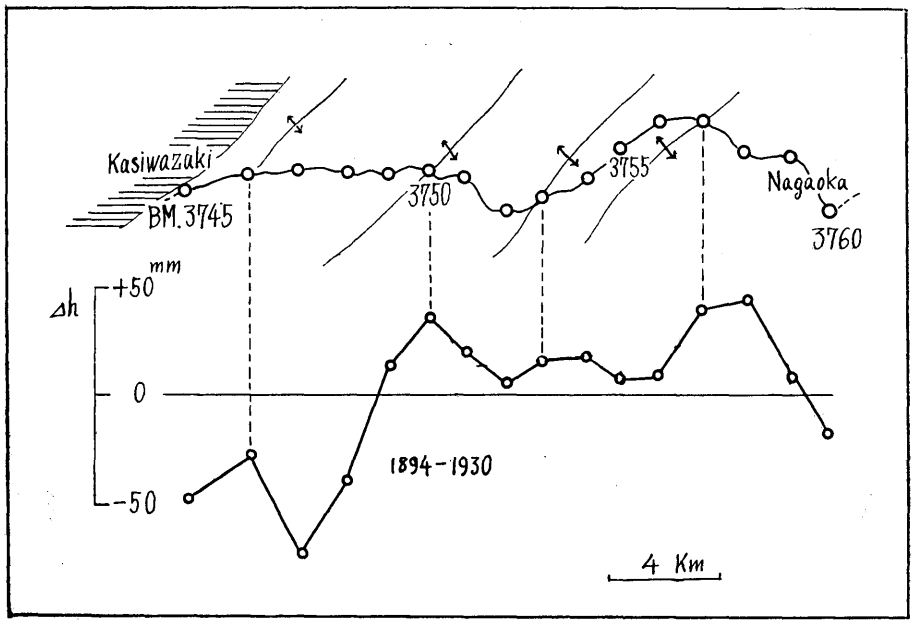

Fig. 6. Example of active folding along the route from Kasiwazaki to Nagaoka, Niigata Pref.

15) Y. OTUKA, *Tisitukôzô to Sono Kenkyû* (1952), 174-186.
16) G. S. I., *Niigata-tihô Zibanhendô Tyôsa* (1960), 13-19.
17) *loc. cit.*, 16).

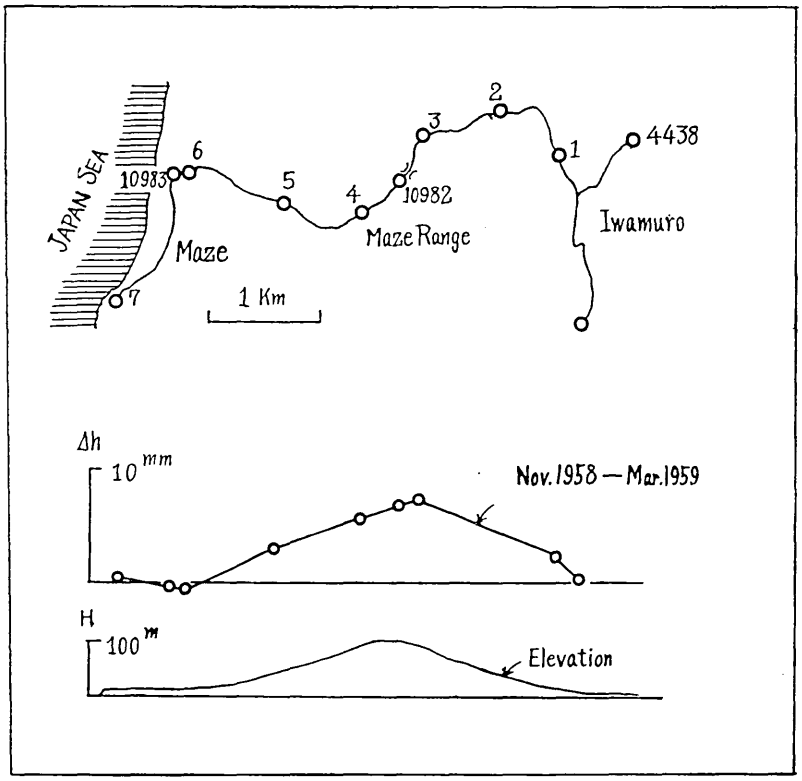

Fig. 7. Example of small scale warping along the levelling route of bench marks from Iwamuro to Maze, Niigata pref.

2) *Activity of fault*

Formation of fault structure has been investigated from both the geological and geophysical aspects. It has been known that there are generally two cases of active faults:

(1) The displacement of the ground on both sides of the fault advances in the directions respectively in which the ground displaced when the fault is formed.

(2) The displacements go in the directions opposite to those in the case above.

Both the faults have an important bearing on the geophysical study of crustal deformation. A number of studies in this line[18] have been made in Japan on the basis of the results of precise geodetic observation.

18) K. KASAHARA, "The Nature of Seismic Origin as Inferred from Seismological and Geodetic Observation (I)", *Bull. Earthq. Res, Inst.*, **35** (1957), 512-523.

3) *Secular subsidences*

As has already been mentioned, subsidence of the crust is essentially different from mere compaction of the alluvial plane. The author would here like to discuss subsidence due to deformation or tilting of the earth's crust. The amount of displacement actually observed consists of pure crustal deformation and earth compaction so that it is difficult, in general, to separate the deformation exactly. We can recognize, however, the general tendency of crustal deformation if we make use of results of geodetic survey covering a large area.

According to the results of the precise levelling surveys over the Island arc of Japan, secular tilting motions have been clearly revealed at some places along the coast line in the south-western part of Japan facing the Pacific Ocean. There is a marked contrast between sudden upheaval associated with great earthquakes and secular subsidence over a period during which no great earthquake occurred as has been found at the Kii peninsula and Muroto promontory.

We obtain the following relation between the tilting angle (φ) and the direction of maximum slant ($\theta_{\max}$), ($\varphi_{\max}$) being then obtained by means of the least square method for φ and θ [19]

$$\varphi=\varphi_{\max}\sin(\theta_{\max}-\theta) \tag{1.2}$$

where

φ: tilting angle between the bench marks. Denoting the relative vertical displacement of bench marks by Δh and the distance between them by S, φ is given as

$$\varphi\fallingdotseq\tan\varphi=\Delta h/S \quad \text{(radian)}$$

$\varphi_{\max}$: the angle of the inclination along the maximum tilting axis.

$\theta_{\max}$: the azimuth of the maximum tilting axis.

θ: the azimuth of the line connecting two bench marks.

According to this formula, the subsidence at the Muroto point is shown in Fig. 8 taking θ as the abscissa.

The sinusoidal distribution of the points in the figure indicates that a large mass of the earth's crust is tilting as one block. $\theta_{\max}$ and $\varphi_{\max}$ are obtained as

$$\theta_{\max}=\text{N }10^{\circ}\text{W}, \quad \varphi_{\max}=-1.4'' \tag{1.3}$$

19) *loc. cit.*, 2).

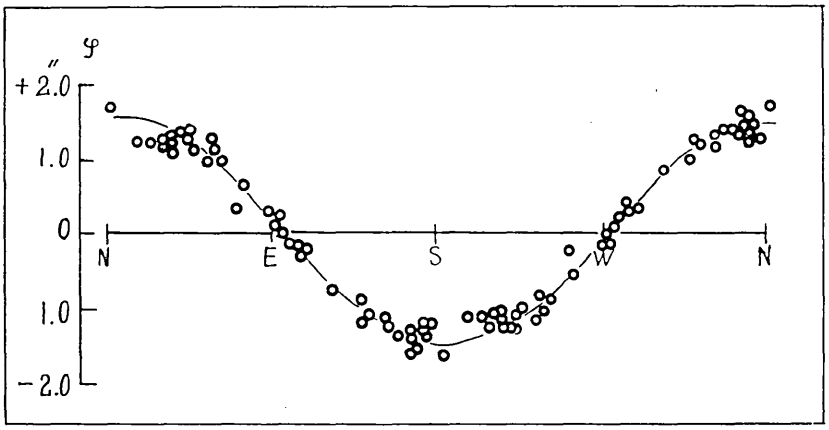

Fig. 8. Tilting along the lines connecting every two bench marks during 1895~1935 period (after Miyabe's sine-method).

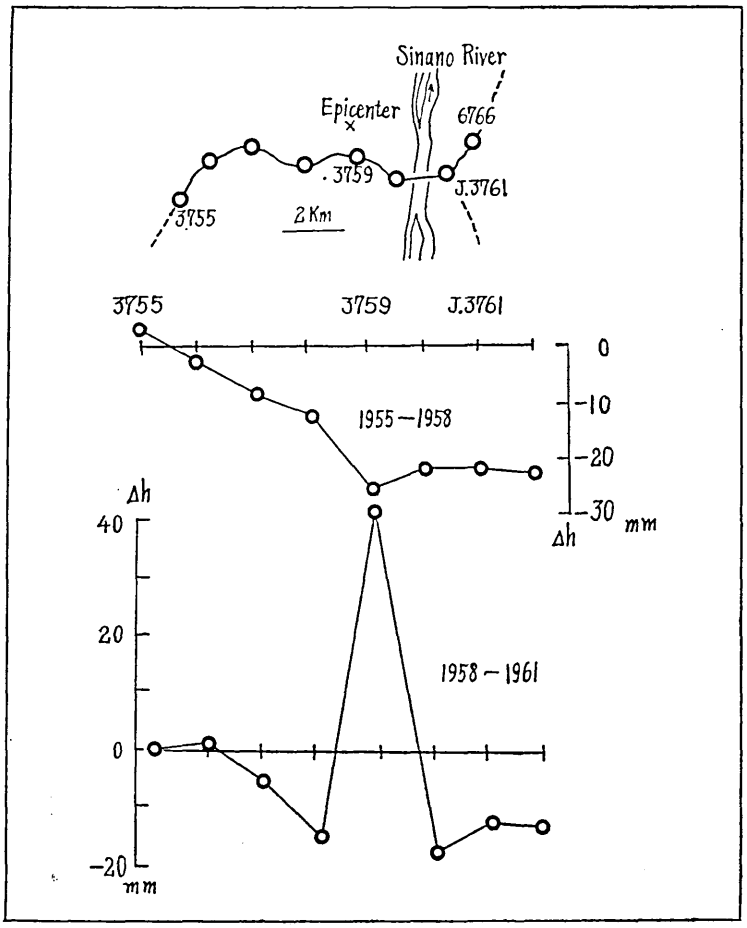

Fig. 9. Vertical displacement of bench marks near epicentral area accompanying with Nagaoka Earthquake (1961. 2. 2), Niigata pref.

We can therefore obtain the constant term in the empirical formula which is mentioned in the previous paragraph, as

$$\varphi_{\max}/t = -0.0348'' . \tag{1.4}$$

Although the relation between secular tilting motion and occurrence of great earthquakes is not made clear yet, it is hoped to conduct further studies for these important and interesting phenomena.

Subsidence in relation to an inland earthquake, is found in the Nagaoka Earthquake[20] on Feb. 2nd, 1961 as shown in Fig. 9. The subsidence should have taken place during a short period from 1955 to 1958. Actually there were upheavals in some parts of the area after the shock.

Chapter 2. Relation between Shallow Earthquake and Upheaval

In this chapter, the relation between dimension of the area of upheaval and vertical displacement is re-examined by analysing results of uplift movement observed by means of precise geodetic levelling for "inland earthquake" in Japan. All the earthquakes whose hypocenters are shallower than 20 km and whose magnitudes are 5.0–7.5 in the Gutenberg-Richter's scale are dealt with. Fig. 10 shows the distribution of shallow earthquakes that have occurred since 1900 in the inland area of Japan causing damage in greater or lesser degree[21]. Taking six earthquakes of which vertical displacements were accurately observed, the relation between the distribution of the vertical displacement and their epicenter is going to be examined here.

§ 1. Distribution of Displacement Accompanied by Shallow Earthquakes in the Area of Upheaval

Many destructive earthquakes had occurred in the inland area of Japan, most of them being so-called "very shallow earthquake" whose magnitudes are larger than 5.0 (Gutenberg-Richter's scale). Nothing regular has been known about the geographical distribution and periodicity of occurrence of these earthquakes. All we can say is that there seem to exist some active seismic zones.

20) A. OKADA, "Land deformation accompanying with Nagaoka Earthquake, Feb. 2nd, 1961.", *Bull. Earthq. Res. Inst.*, **39** (1961), 537-547.

21) J. M. A., *Catalogue of Major Earthquakes which occurred in and near Japan* (1926-1956), 19-91.

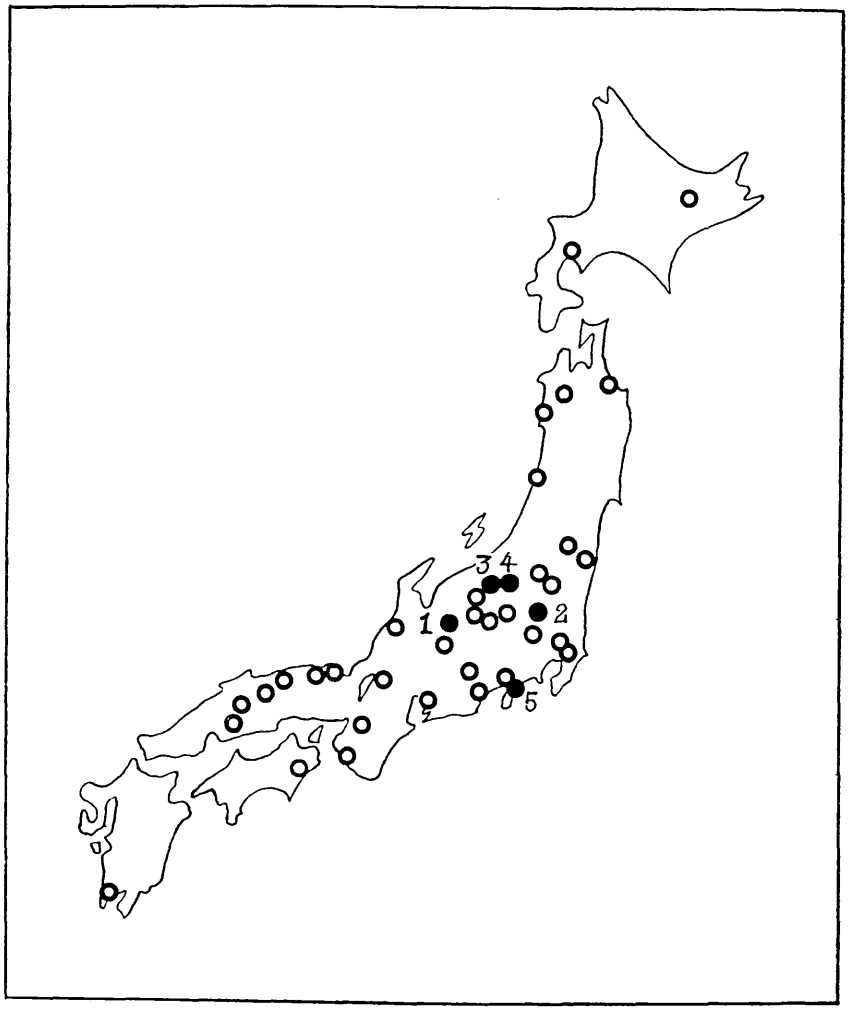

● Uplift observed by precise levelling
1. Ômati 2. Imaiti 3. Sekihara 4. Nagaoka 5. Itô

Fig. 10. Distribution of shallow earthquakes accompanying damage during the period 1900～1961. Magnitude (Gutenberg-Richter's scale)≥5.0, Depth≤20 km. (after Rika Nemppyô and JMA Catalogue)

Vertical displacement associated with the earthquakes was made clear only for half of them because the levelling route did not always cover the respective areas. Excluding the earthquakes that are accompanied by faults on the ground surface, upheaval movements are examined using the results of the precise levelling. The relative position

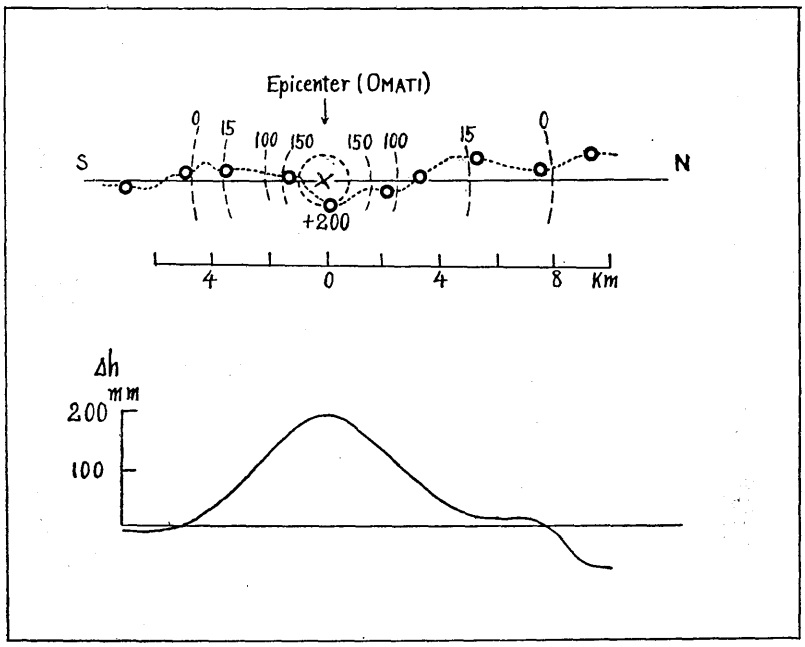

Fig. 11. Distribution of surface vertical displacement, Ômati Earthquake.

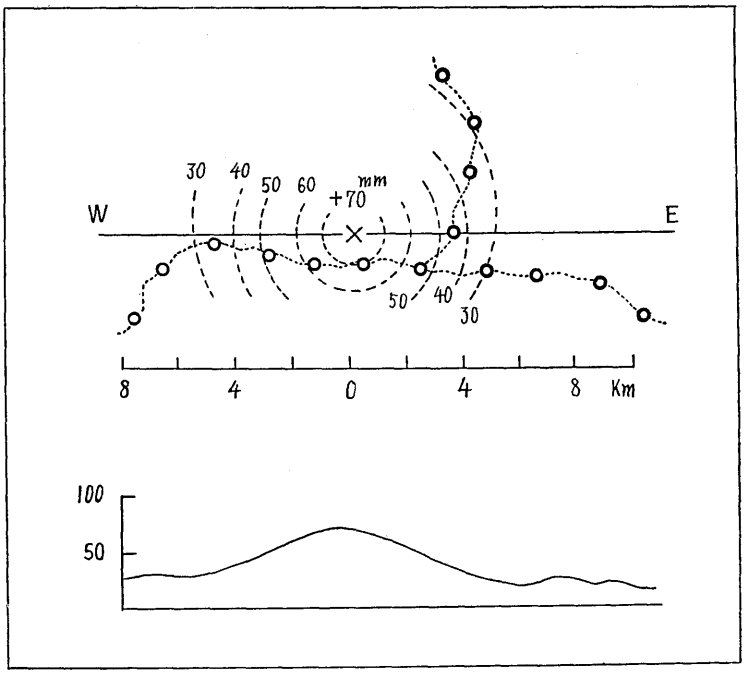

Fig. 12. Imaiti Earthquake.

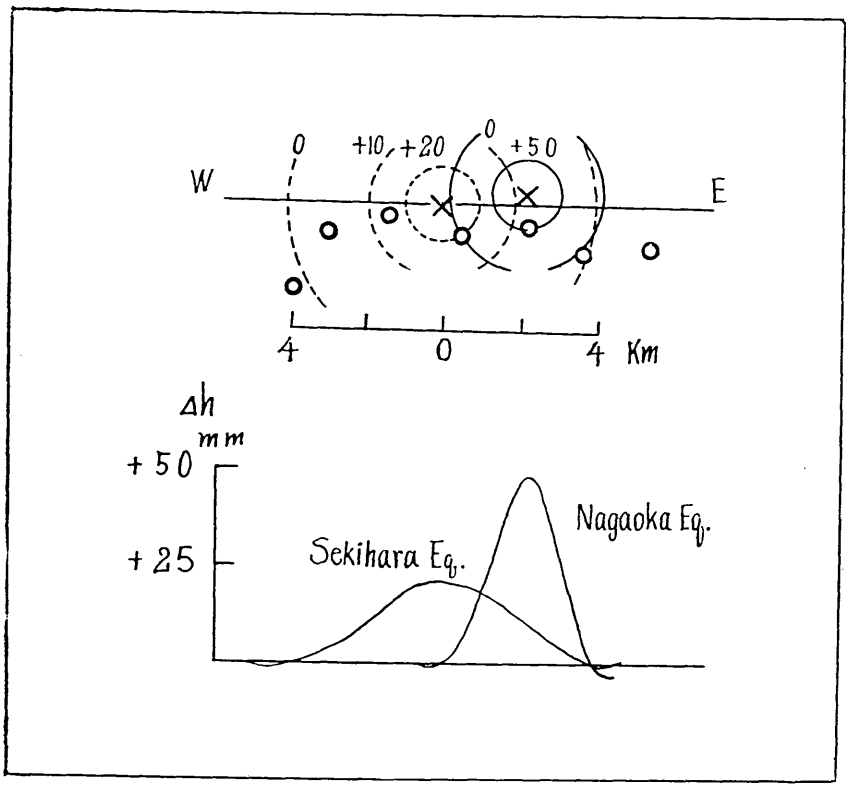

Fig. 13. Sekihara and Nagaoka Earthquakes.

of epicenters and distribution of vertical displacement may be easily obtained on the map as is demonstrated in the following. Figs. 11–13 show profiles of vertical displacement for a few earthquakes. In the case of the Ômati Earthquake, the profile of the vertical displacement is somewhat assymmetric with the epicenter as shown in Fig. 11; nevertheless we may assume that the profile is symmetric for the first approximation. From the profiles of the Imaiti, Sekihara and Nagaoka Earthquakes shown in Fig. 12 and 13 respectively, we may also assume, to some degree of approximation, that the vertical displacement is distributed symmetrically.

The distance (R) between the epicenter and the surrounding area where the vertical displacement is reduced to zero amounts to about 5–6 km. In Figs. 11–13, the top figure shows the levelling route and iso-upheaval diagrams, the middle the scale of distance, and the lowest the profile of the displacement diagrams, and all are projected on the plane

which is parallel to the levelling route passing the epicenter.

Fig. 14 shows the position of bench marks and epicenters for the Itô Earthquake swarm as well as the vertical displacement of bench

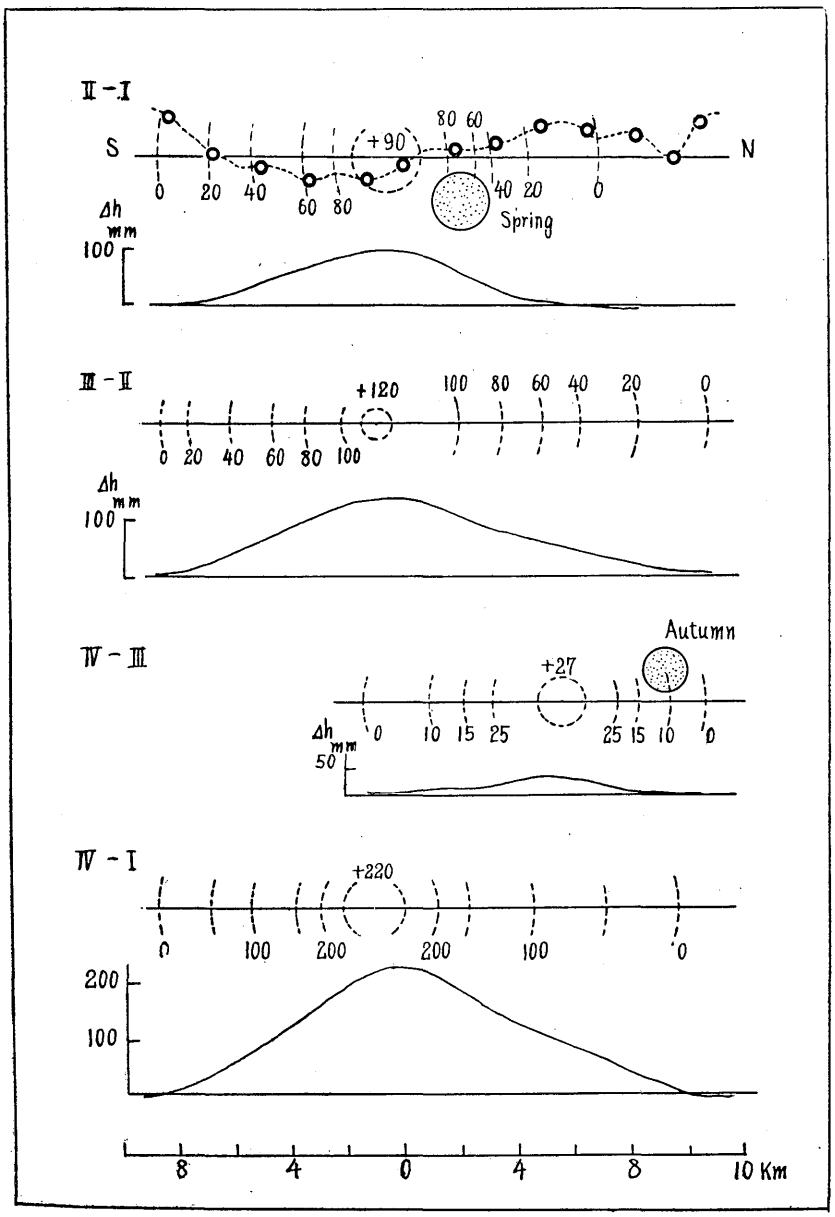

Fig. 14. Itô Earthquake swarm (in each stage).

marks. In this case the precise levelling surveys were repeated four times during a period of half a year. Although we found some discrepancy between the epicenter and the location of the maximum displacement, it might be possible to ascribe this to the shifting of the hypocenter of the swarm earthquakes.

From the above considerations, in the case of destructive earthquakes, of magnitude 5.0–6.0 and hypocenter less than 10 km in depth, it would not be impossible to take typical values for $\delta h_{\max}$ and $R_{\max}$ as 20 cm and 10 km respectively.

§ 2. Relation between Vertical Displacement and Depth of Hypocenter

In order to analyse the displacements brought forth in the last section, we take an assumption that the deformation is caused by the pressure increase in a sphere supposed at the hypocenter, while the earth's crust is regarded as a semi-infinite elastic medium. Denoting the vertical displacement by $\bar{u}_z$, the horizontal one by $\bar{u}_R$ and the rotation by $\bar{u}_\phi$, we can express the displacement as follows[22],

$$\left.\begin{aligned} \bar{u}_z &= -\frac{3\alpha^3 p}{4\mu}\int_0^\infty k e^{-kf} J_0(kR)dk \\ \bar{u}_R &= -\frac{\alpha^3 p}{4\mu}\int_0^\infty k e^{-kf} J_0'(kR)dk \\ \bar{u}_\phi &= 0 \end{aligned}\right\} \tag{2.1}$$

where

α : radius of sphere
p : pressure increase
f : depth of center of sphere
R : horizontal distance from epicenter.

Since no observations of horizontal displacement on the earth's surface are available, we are obliged to develop the theory only from the vertical displacement U_z on the surface, the value of U_z being given as[23]

$$U_z = \bar{u}_z = -\frac{3\alpha^3 p}{4\mu}\frac{f}{(f^2+R^2)^{3/2}}. \tag{2.2}$$

22) N. YAMAKAWA, "On the Strain Produced in a Semi-infinite Elastic Solid by an interior source of Stress", *Zisin*, **8** (1955), 84-98.

23) K. MOGI, "Relation between the Eruptions of Various Volcanoes and the deformations of the Ground Surface around them", *Bull. Earthq. Res. Inst.*, **36** (1958), 99-134.

We then see that the distribution of the vertical displacement is given as a function of α (radius of sphere), p (pressure increase), f (depth of hypocenter) and R (horizontal distance from epicenter).

If we assume

$$\alpha^3 p = k \quad (k: \text{constant})$$

U_z is the quantity to be determined by f and R. The formula is written as

$$U_z = k \frac{1}{f^2\{1+(R/f)^2\}^{3/2}} \,. \tag{2.3}$$

Fig. 15 is the diagram for the vertical displacement U_z as a function of R as derived from the formula (2.3) taking f as the parameter.

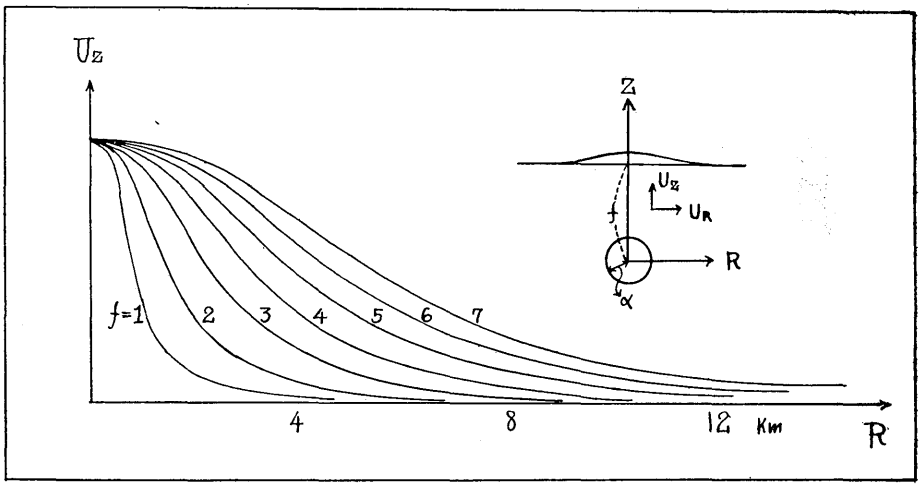

Fig. 15. Calculated curves of the vertical displacement (U_z) versus the radial distance (R).

If the upheaval of the earth's crust is caused by a pressure increase in a sphere, as has been assumed in the beginning of the theory, it is possible to presume f by comparing the observed distribution with the curves in Fig. 15. It is not always possible to determine one value for f because the curve actually observed has a shape slightly different from the theoretical ones. In such a case, only the possible range of f is to be determined. The values of f are determined for each earthquake concerned and are listed in Table 1.

Table 1. Shallow earthquakes accompanied by upheaval.

No.	Name	M	Date	δh_{max}	H	f	Remark
				cm		km	
1	Ômati Earthquake	6.1	Nov. 11th, 1918	20	—	4~6	24),25),26)
2	Imaiti Earthquake	6.5	Dec. 26th, 1949	7	*vs*	5~6	27)
3	Sekihara Earthquake	5.4	Oct. 27th, 1927	2	10	1~3	28)
4	Nagaoka Earthquake	5.0	Feb. 2th, 1961	5	10	1~3	29)
5	Itô Earthquake swarm	4.3~5.2	Apr.~Nov. 1930	2~20	10	4~7	30)

M: Gutenberg-Richter's Magnitude
H: Depth (Seismometrical)
f: Depth of sphere

1) *Ômati Earthquake*

The Ômati Earthquake is one of the most typical examples of the upheaval of the earth's crust accompanied by an earthquake. The bench marks on a levelling route passing through the epicentral area from the

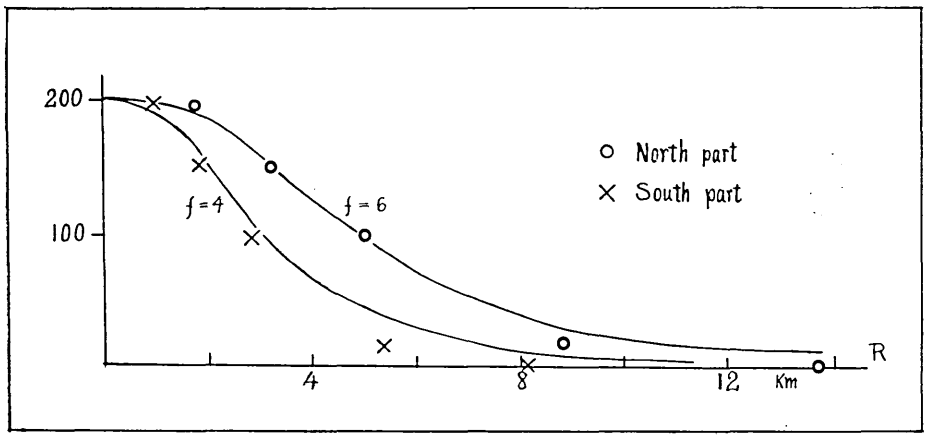

Fig. 16. Ômati Earthquake.

24) F. ÔMORI, "Taishô 7nen Ômati-tihô gekisin tyôsahôkoku" (I), *Rep. Imp. Earthq. Invest. Comm.*, **94** (1921), 39-46.

25) F. ÔMORI, "Taishô 7nen Sinano-Ômachi-tihô gekisin tyôsahôkoku" (II), *Rep. Imp. Earthq. Invest. Comm.*, **98** (1922), 23-31.

26) S. TSUBOI, "Shinshû Ômati-Zishin tyôsa gaiyô," *Rep. Imp. Earthq. Invest. Comm.*, **98** (1922), 13-31.

27) G. S. I., *Compilation of the 1st order precise levelling resurvey (Ittô Suijunten, Kensoku Seika Syûroku)*, Vol. 1 (1955), 25-9.

28) *loc. cit.*, 1).

29) *loc. cit.*, 20).

30) *loc. cit.*, 1).

north to the south showed the maximum upheaval of 200 mm at the point in Ômati city and the distribution of the vertical displacement extended symmetrically along the levelling route.

Now, in the northern part of the route, the profile of the vertical displacements fits in to the calculated curve for $f=6$ km, while in the southern part the profile fits in to the curve for $f=4$ km. The depth of the hypocenter is therefore presumed to be about 4–6 km.

2) *Imaiti Earthquake*

Fig. 17 shows the example at the time of Imaiti Earthquake. The profile of the vertical displacement curves for $f=5$–6 km. In this case the depth of the hypocenter is about 5–6 km.

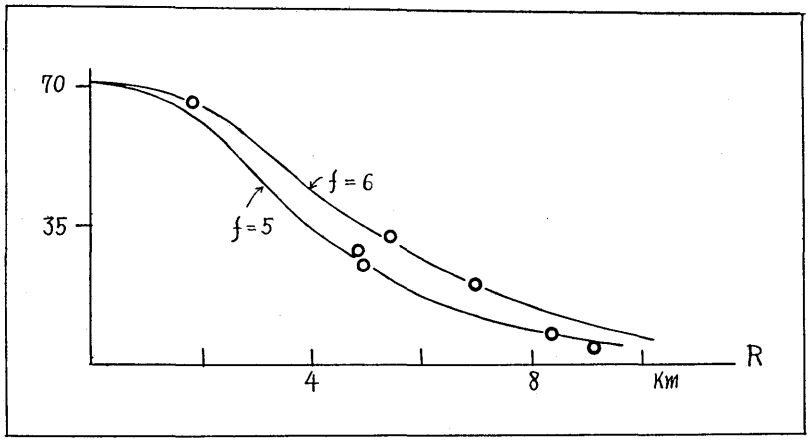

Fig. 17. Imaiti Earthquake.

3) *Sekihara and Nagaoka Earthquake*

Fig. 18 shows examples for the Sekihara and Nagaoka Earthquakes, their epicenters close to one another as shown in Fig. 13. The values of f are estimated as 1–3 km for the Sekihara and Nagaoka Earthquakes. Thus the results may provide a proof that the hypocenters of these earthquakes are very shallow.

4) *Itô Earthquake Swarm*

The Itô Earthquake Swarm is well known because of its particular mode of occurrence of many minor earthquakes. During the active period of earthquake swarm, a number of levelling surveys were carried out repeatedly, so that the upheaval movement was traced from time

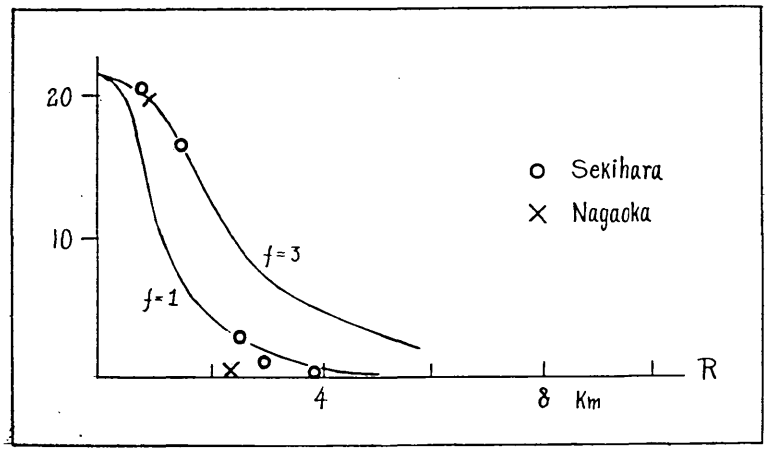

Fig. 18. Sekihara and Nagaoka Earthquakes.

to time. The changes in the height of each bench mark obtained through four surveys are shown in Fig. 14, where the epicentral regions for the two groups were determined by seismometrical observation. One represents the earthquake swarm in the Spring and the other in Autumn of 1930.

The epicentral area does not agree with the center of upheaval zone in this example. If it be assumed, however, that the pressure source is situated beneath the ground surface near the maximum displacement area, the depth f could be obtained as follows. (Fig. 19) In this way the depth of the hypocenter is estimated at about 4–5 km. During the IV-I interval when the earthquake swarm continued, the value of f (depth) is 5–7 km.

By the above method, we obtain in every case hypocenters shallower than the ones determined seismometrically. A cause of this discrepancy may be due to the non-elastic deformation at the surface of the earth's crust, that is, the thickness of the weathering layer or alluvial plane. Even if we assume a surface layer 1 km in thickness the depth of hypocenter (f) is much smaller than the one obtained by the seismometrical method (H).

§ 3. Energy of Shallow Earthquakes Presumed from Analysis of Vertical Displacement

In the previous section, a pressure increase in a sphere buried in a semi-infinite elastic medium was assumed. Although the depth of the

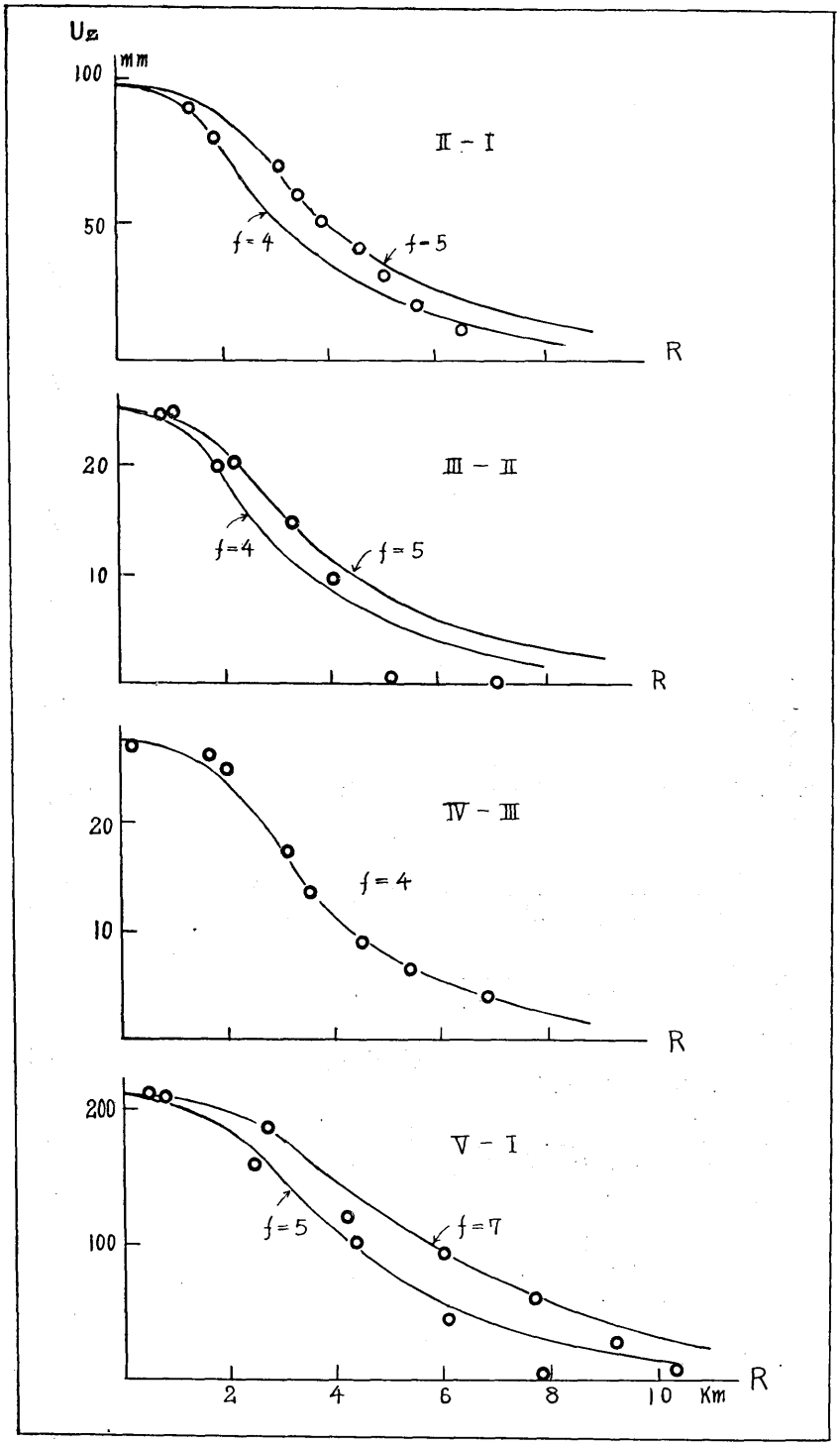

Fig. 19. Itô Earthquake swarm.

sphere could be inferred by comparing the observed vertical displacements with the theoretical ones, the term $\alpha^3 p$ (pressure increase) has been left unknown. When the pressure increases, the radius of the sphere changes from α to α'. Accordingly, the surface of the semi-infinite medium would change from the full line to the dotted line as schematically shown in Fig. 20. The horizontal and vertical displacements at any point are given as[31]

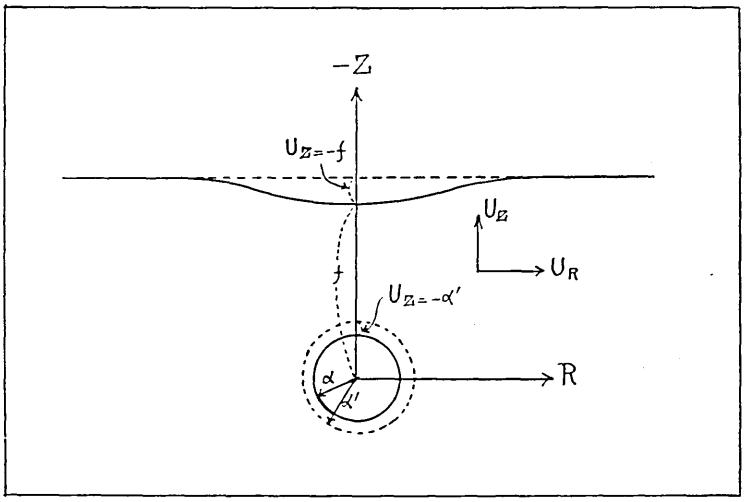

Fig. 20. Model of pressure increase in an underground in the semi-infinite elastic medium.

$$\left.\begin{aligned} U_R &= -\frac{\alpha^3 p}{4\mu}\frac{R}{\{(z+2f)^2+R^2\}^{5/2}}(5z^2+14fz+8f^2-R^2) \\ &\quad +\frac{\alpha^3 p}{4\mu}\left[\frac{z}{(z^2+R^2)^{3/2}}+\frac{R}{\{(z+2f)^2+R^2\}^{3/2}}\right] \\ U_z &= \frac{\alpha^3 p}{4\mu}\frac{1}{\{(z+2f)^2+R^2\}^{5/2}}(7z^3+38fz^2+68f^2z+4f^3+4fR^2+zR^2) \\ &\quad -\frac{\alpha^3 p}{4\mu}\left[\frac{z}{(z^2+R^2)^{3/2}}-\frac{z+2f}{\{(z+2f)^2+R^2\}^{3/2}}\right] \end{aligned}\right\} \quad (3.1)$$

where α: original radius of sphere
p: pressure increase
f: vertical distance from top to center of sphere
R: horizontal distance

31) *loc. cit.*, 23).

λ, μ : elastic constant
U_R : displacement in R-direction
U_Z : displacement in Z-direction.

As we cannot easily detect horizontal displacement, the following theory is based only on vertical displacement which is determined by means of precise levelling surveys. The vertical displacements on the Z-axis at points $R=0$ km, $Z=-f$ km and $R=0$ km, $Z=-\alpha'$ km are given as

$$\left.\begin{aligned} U^0_{Z=-f} &= \frac{3\alpha^3 p}{4\mu}\frac{1}{f^2} \\ U_{Z=-\alpha'} &= \frac{\alpha^3 p}{4\mu}\left[\frac{(3f-2\alpha')}{(2f-\alpha')^3}+\frac{1}{4\alpha'^2}\right] \end{aligned}\right\}. \tag{3.2}$$

From (3.2) we can get

$$U_{Z=-\alpha'}/U^0_{Z=-f} = \frac{4f^2}{3}\left[\frac{(3f-2\alpha')}{(2f-\alpha')^3}+\frac{1}{4\alpha'^2}\right]. \tag{3.3}$$

In formula (3.3), the term $U^0_{Z=-f}$ on the left-hand side (displacement of the free surface) is derived from the results of levelling survey. We can then estimate the displacement at the surface of the sphere provided the ratio of f to α' are given. If α' is assumed as

$$f/2>\alpha'>f/4 \tag{3.4}$$

we get

$$U/U^0 \fallingdotseq 2\sim 6\ .$$

So we see that the displacement at the surface of the sphere on Z-axis is 2–6 times as large as that at the ground surface. The depth f having been estimated in the previous section, we can approximately presume the possible range of α' as long as condition (3.4) holds good. If we assume that an earthquake occurs when the strain caused by the pressure exceeds the strength of material and that the preseismic equilibrium state is recovered, the total energy released is given as

$$E=p\pi\alpha'^2 U_{Z=-\alpha'} \tag{3.5}$$

where α' : radius of sphere
$U_{Z=-\alpha'}$: displacement on surface of sphere
p : hydrostatic pressure increase in sphere.

On the other hand, the potential energy and elastic wave energy are calculated independently with the aid of the following formulas respectively.

$$\left.\begin{aligned} E_p &= \frac{1}{3}\pi R^2 U^0_{Z=-f}\rho g h \\ E_e &= 10^{11.8+1.5M} \end{aligned}\right\} \tag{3.6}$$

where R: radius of upheaval area
$U_{Z=-f}$: vertical displacement at $R=0$ km
ρ: density (2.0 assum)
h: depth
M: Gutenberg-Richter's magnitude.

The first formula in (3.6) is derived by assuming that the vertical displacement changes linearly between $R=0$ and $R=R$, the displacement vanishing at the latter distance.

The strain energy accumulated in the sphere would be released mainly as potential energy and elastic wave energy at the time of earthquake, so that we may put

$$E=E_p+E_e\,. \tag{3.7}$$

Substituting (3.5) and (3.6) into (3.7). We get

$$p=\left(\frac{1}{\pi\alpha'^2 U_{Z=-\alpha'}}\frac{1}{3}\pi R^2 U_{Z=-f}\rho g h + 10^{11.8+1.5M}\right). \tag{3.8}$$

Since all the terms on the right-hand side of the expression can be inferred by seismometric and geodetic means, the increase in hydrostatic pressure in the sphere can be estimated for each earthquake. The increases in hydrostatic pressure thus calculated for the respective earthquake are shown in Table 2 together with the E_p and E_e.

If we assume that the upheavals associated with earthquakes are simply caused by pressure increases without any rupture, it is obvious that the pressure increase in this case is given as

$$P'_{(\text{statical})}=\frac{4\mu U^0_Z f^2}{3\alpha^3} \tag{3.8}$$

where $\mu=10^{11}$
$f=4\alpha$ (assum.)
U^0_Z=maximum displacement.

The P' (static) values calculated in this way are also given in Table 2. Insofar as we assume that the origin of inland shallow earthquakes is an increase in hydrostatic pressure in a sphere buried in a semi-infinite medium, the pressure increase sufficient to explain the upheaval observed is estimated at 100–300 atm.

Table 2. List of calculated energy and estimated pressure of increase.

No.	Name	f	R	$U^0_{Z=-f}$	$U_{Z=-\alpha}$	α'	M	E_e
		km	km	cm	cm	km		erg
1	Ōmati	5	5	20	60	1.25	6.1	$10^{20.95}$
2	Imaiti	6	5	7	21	1.5	6.5	$10^{21.56}$
3	Sekihara	2	4	2	6	0.5	5.4	$10^{19.90}$
4	Nagaoka	1.5	2	5	15	0.4	5.4	$10^{19.30}$
5	Itô (total)	6	10	20	60	1.5	5.8	$10^{20.50}$

No.	Name	E_p	E	P	P'	Remark
		erg	erg	dyne/cm^2	dyne/cm^2	
1	Ōmati	2.6×10^{21}	$p\times1.2\times10^{13}$	2.2×10^{8}	3.2×10^{8}	$U/U^0=3.0$, $f=4\alpha'$ assum.
2	Imaiti	1.1×10^{21}	$p\times0.6\times10^{13}$	1.8×10^{8}	1.0×10^{8}	〃
3	Sekihara	1.7×10^{19}	$p\times3.7\times10^{11}$	0.5×10^{8}	0.9×10^{8}	〃
4	Nagaoka	3.3×10^{19}	$p\times1.1\times10^{11}$	3.0×10^{8}	2.3×10^{8}	〃
5	Itô (total)	2.5×10^{22}	$p\times1.7\times10^{13}$	1.5×10^{8}	2.9×10^{8}	〃

E_e: energy of elastic wave
E_p: potential energy
E : elastic strain energy
P : increased hydrostatic pressure
P': $4\mu U^0_{Z=-f}/3\alpha^3$, ($\mu=10^{11}$ assum.)
M : Gutenberg-Richter's Magnitude

Chapter 3. Correlation between Secular Crustal Deformation and Gravity Anomaly

Various aspects of secular crustal deformation have been brought to light throughout Japan with the developement of geodesy. Although a great store of evidence relating to vertical displacement has been obtained by means of precise levelling survey up to the present time, this data can only provide knowledge of relative movement. It is impossible to set a datum point which does not displace with reference to a coordinate system fixed to the earth, only from levelling. The datum could be obtained by reference to the secular mean sea level.

The observation of the mean sea level is carried out by mareographs though the accuracy of observation is inevitably lower than of precise levelling. Disturbances induced by variations of the sea condition give rise to complicated irregularities of the mean sea level. It is then customary to set an approximate datum point from the observation of the secular mean sea level determining the crustal movement. Fortunately tilting motion, that is determined by the relative vertical displacement of bench marks, is free from the errors in the determination of the datum point.

In this chapter, we compare the secular upheaval of the huge area in Fennoscandia with the secular subsidences in Japan considering the correlation between the gravity anomaly and the annual mean velocity of crustal movement in these regions.

§ 1. Relation between Annual Mean Velocity of Depression and Gravity Anomaly along the Coast-line in South-western Japan

The characteristic features of the crustal movement of the Kii peninsula and the Muroto promontory in the south-western part of the Median line are shown Fig. 21. In the figure, the dotted lines show the nodal lines on which vertical displacement takes place at the time of great earthquakes. It can be said that these lines approximately agree with the nodal line for the secular vertical displacement.[32),33)] In Fig. 22, we can see the detail of the vertical displacement along the coast of Sikoku Island during periods 1894–1927 and 1927–1947 respectively, while similar curves for the vertical displacement along the coast of Kii peninsula are shown in Fig. 23. Recently, a gravity survey[34)] was carried out along the levelling routes, so that we can study how the vertical displacements of bench marks can be correlated to the gravity anomaly which is also shown in Figs. 22 and 23. The relation between the gravity anomaly $\Delta g_0''$ and mean velocity ∂h mm/year of subsidence at each bench mark along the routes running south of the nodal lines in both the peninsulas is illustrated in Figs. 24 and 25. As a matter of

32) *loc. cit.*, 27).

33) T. OKUDA, "On the Mode of the Vertical Land Deformation Accompanying the Great Nankaidô Earthquake 1946," *Bull. Geogr. Surv. Inst.*, **2** (1950), 37–59.

34) C. Tsuboi, et al., "Gravity Survey along the Lines of Precise Levels throughout Japan by Gravimeter, Part. 1, Sikoku District." *Bull. Earthq. Res. Inst.*, Suppl., **4** (1953), Part 1, 18–44.

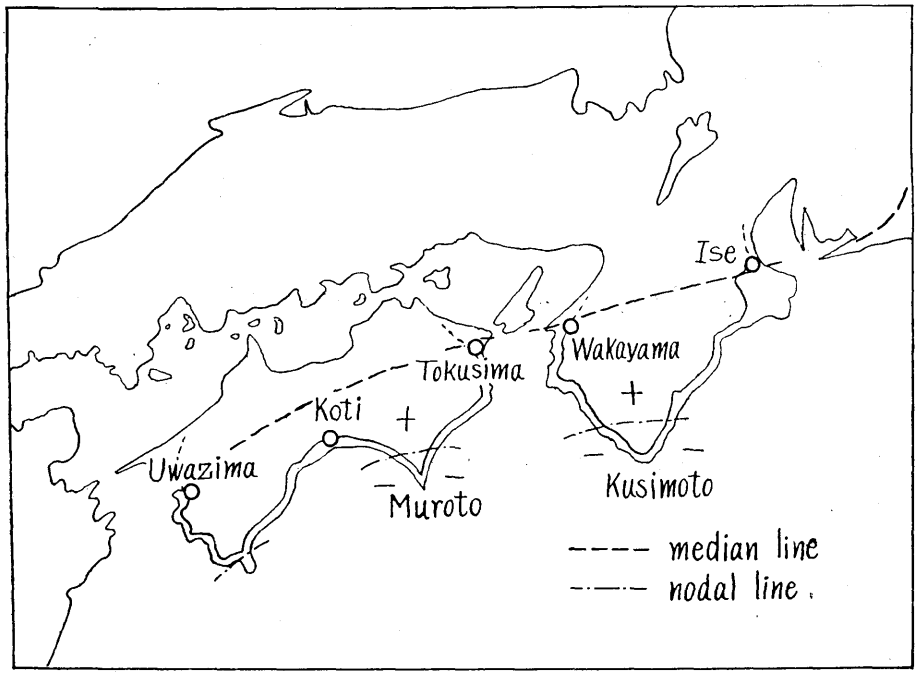

Fig. 21. Distribution of secular earth movement in South-western Japan.

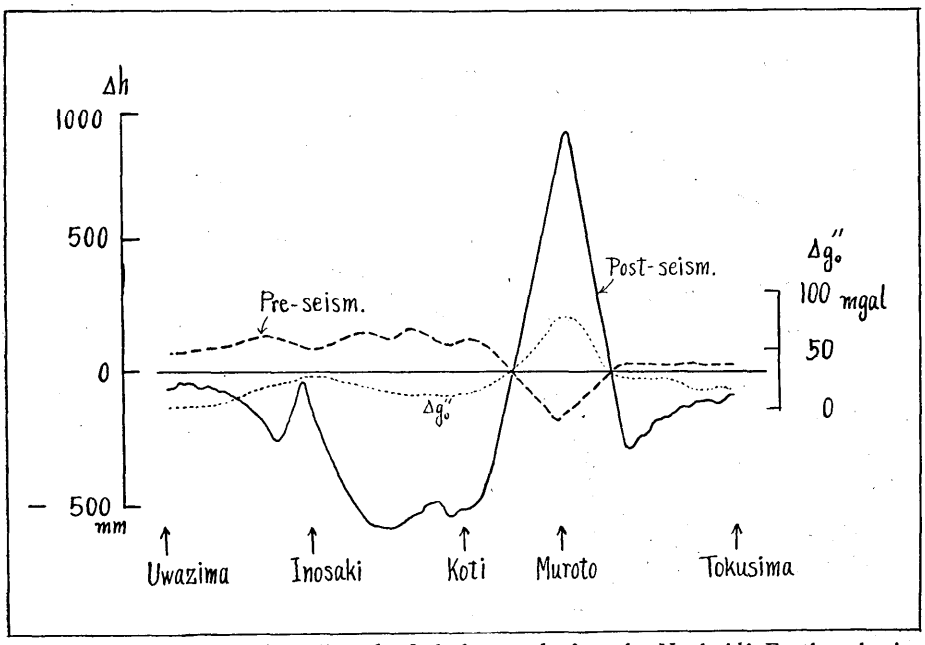

Fig. 22. Diagram of $\Delta g_0''$ and Δh before and after the Nankaidô Earthquake in Shikoku Island.

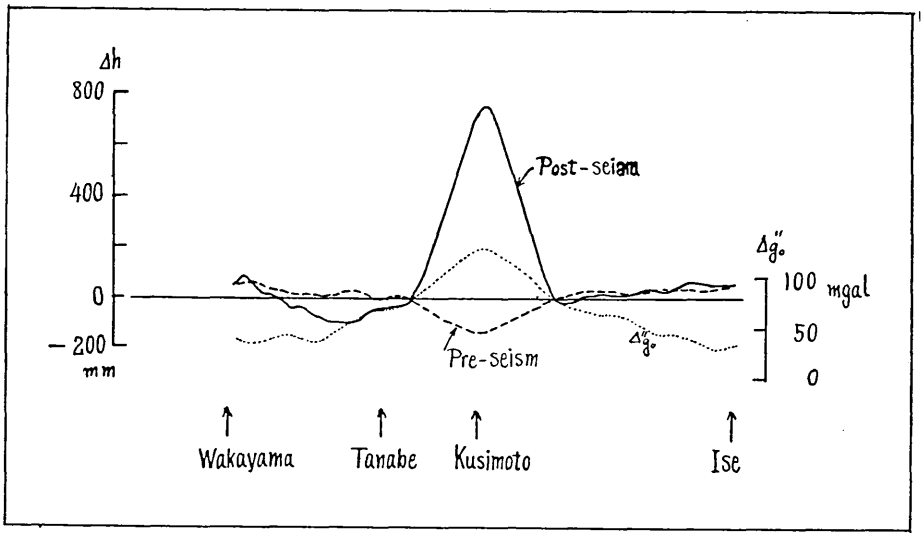

Fig. 23. Diagram of $\Delta g_0''$ and Δh before and after the Nankaidô Earthquake in Kii Peninsula.

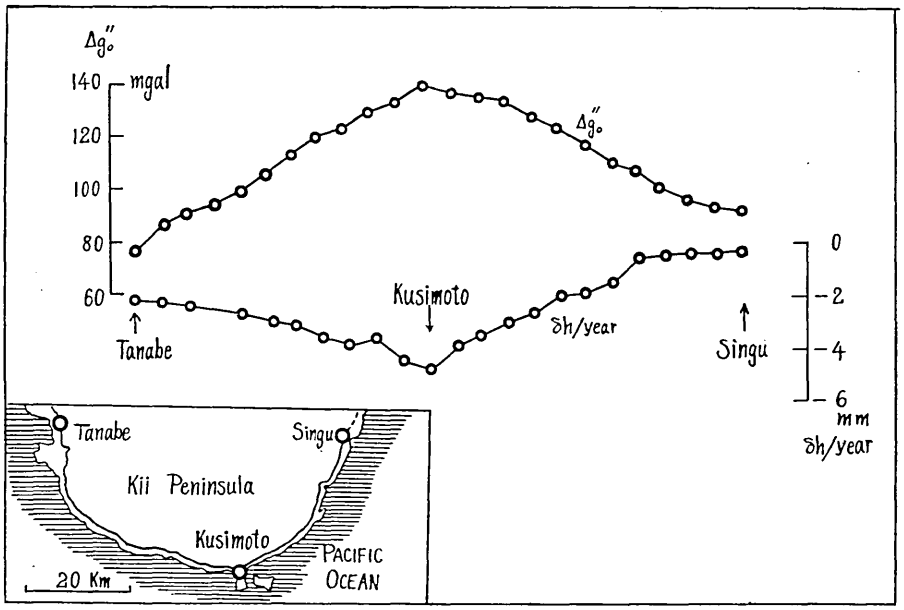

Fig. 24. Diagram of $\Delta g_0''$ and δh/year at each bench mark in the southern part of Kii Peninsula.

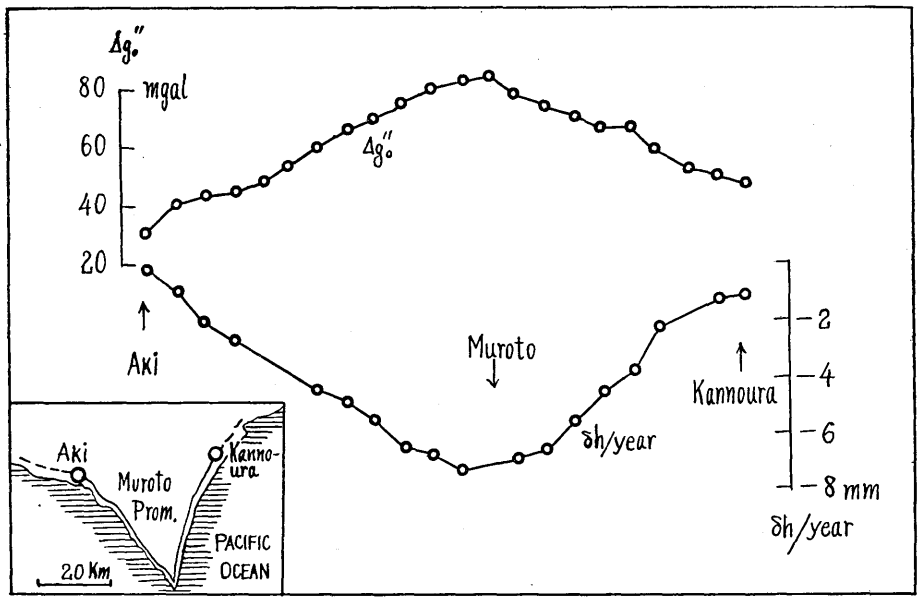

Fig. 25. Diagram of $\Delta g_0''$ and δh/year at each bench mark in Muroto Promontory.

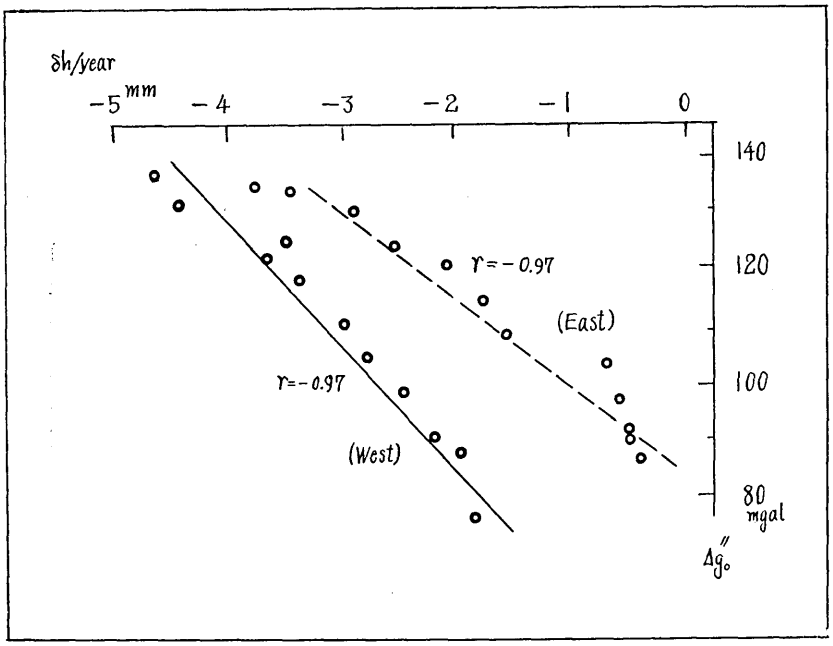

Fig. 26. Diagram of Correlation between $\Delta g_0''$ and δh/year in Kii Peninsula.

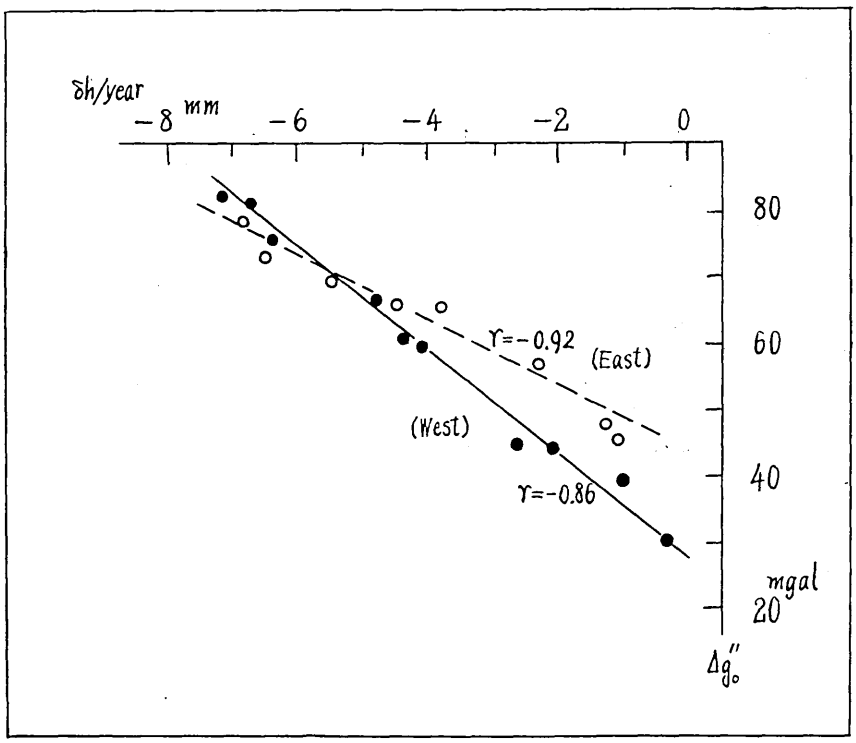

Fig. 27. Diagram of correlation between $\Delta g_0''$ and δh/year in Muroto Promontory.

fact, remarkable resemblance in the $\Delta g_0''-\delta h$ mm/year relation exists between both the regions. It seems to the author that there is a difference in the mode of correlation between the eastern and the western coast lines of both the peninsulas as shown in Fig. 26 and 27. Although no physical meaning for the relation between the annual mean velocity δh mm/year and the gravity anomaly $\Delta g_0''$ is known, we may assume a linear relation as

$$\delta h_j=\overline{\delta h}+\alpha(\overline{\Delta g_0}''-\Delta g_{0j}'')$$

in which α is the regression coefficient, while $\overline{\delta h}$ and $\overline{\Delta g_0}''$ are the values of the mean average respectivelly. Regression coefficient α for each coast line in both the peninsulas, are calculated by the least square method for both the periods during and after the earthquake as given in Table 3.

If we assume that the crustal deformation took place under the same gravity anomaly, the regression coefficient α shows a difference of the order of 10^2 between secular subsidence and sudden upheaval.

Table 3. Regression coefficient between δh and $\Delta g_0''$.

Loc. / α	Kii Peninsula		Muroto Promontory	
	West	East	West	East
Before Earthquake	− 0.046	− 0.069	− 0.191	− 0.095
After Earthquake	+10.80	+14.12	+34.32	+18.85

We therefore see that it would take some 10^2 years to recover the vertical displacement that suddenly takes place at the time of the earthquake provided the rate of secular movement is assumed to be maintained over a long period. It may also be possible to obtain a similar correlation between δh mm/year and $\Delta g_0''$[35] for the Izu, Miura and Bôsô[36] promontories though the geological structures for these districts are not always the same. The correlation between δh mm/year and $\Delta g_0''$ for these districts is shown in Figs. 28–34. Data for the eastern coast line of the Izu promontory is chosen so as to eliminate the influence of the Itô earthquake swarm.

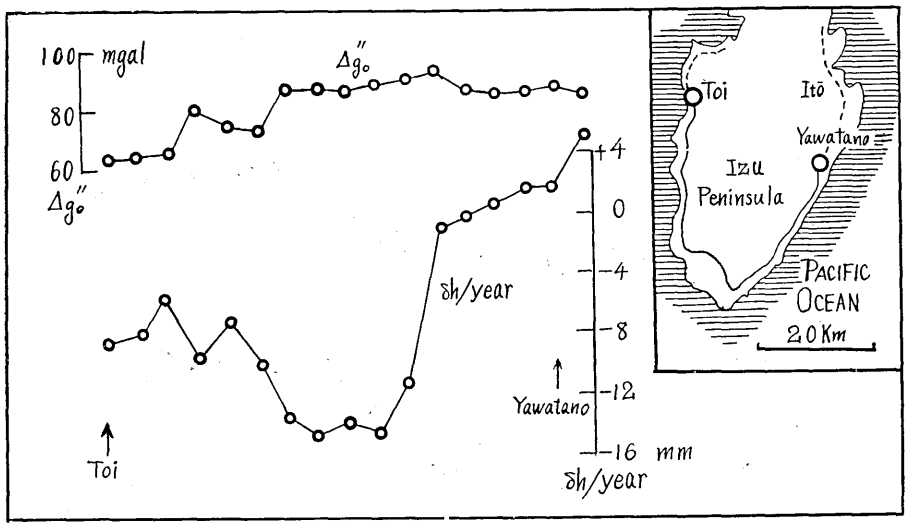

Fig. 28. Diagrams of $\Delta g''$ and δh/year in Izu Peninsula.

35) C. Tsuboi, et al., *loc. cit.*, 34). *Bull. Earthq. Res. Inst., Suppl.* Vol., **4** (1954, 1955, 1956), Part IV 167-197, Part V 301-309, Part VI 371-405, Part VII 461-473, Part VIII 537-551.

36) *loc. cit.*, 1).

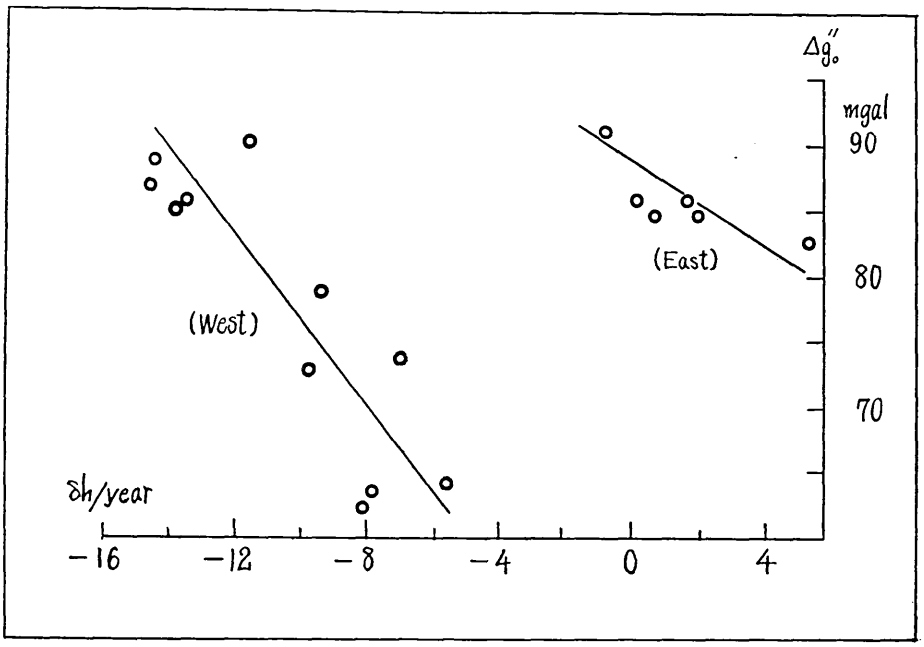

Fig. 29. Diagram of correlation between $\Delta g_0''$ and δh/year in Izu Peninsula.

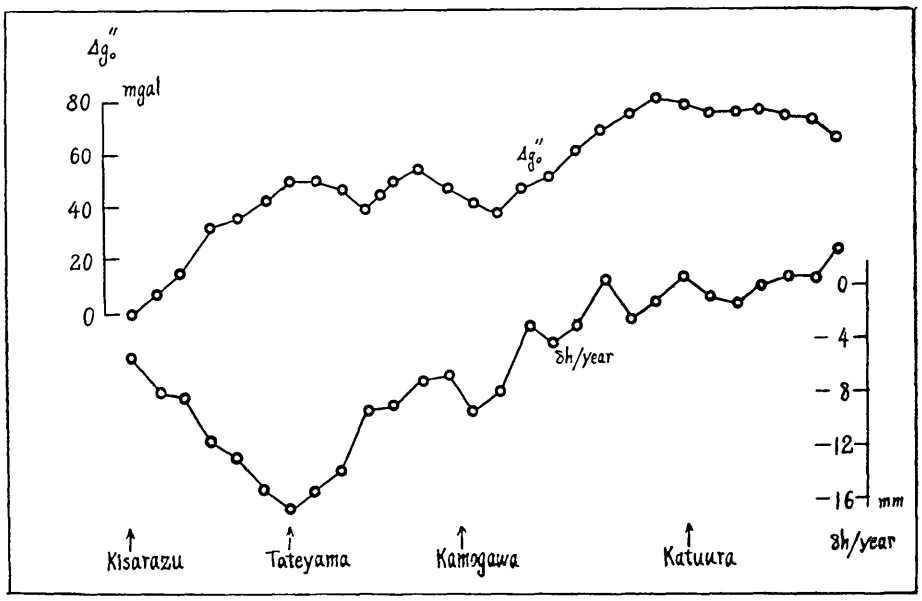

Fig. 30. Diagrams of $\Delta g_0''$ and δh/year in Bôsô Peninsula.

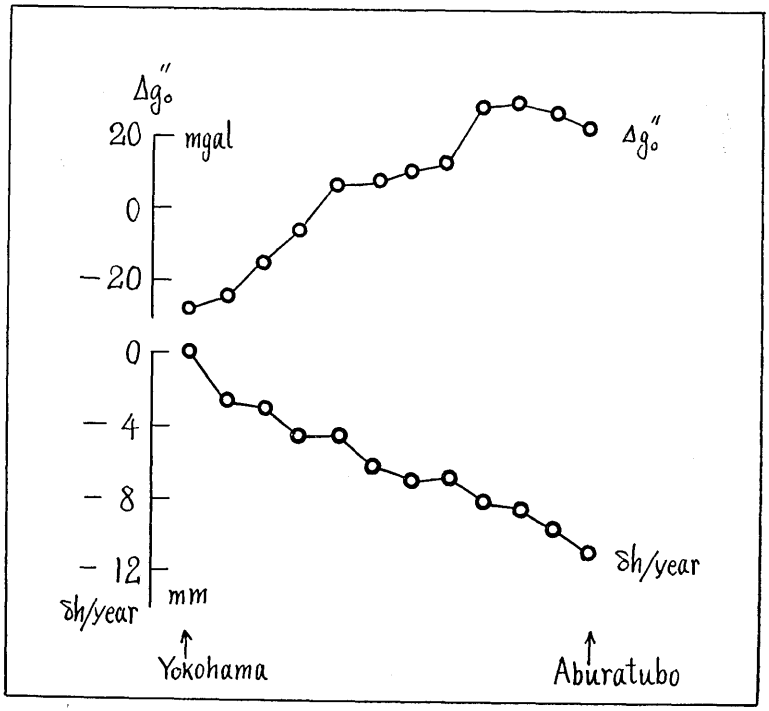

Fig. 31. Diagrams of $\Delta g_0''$ and δh/year in Miura Promontory.

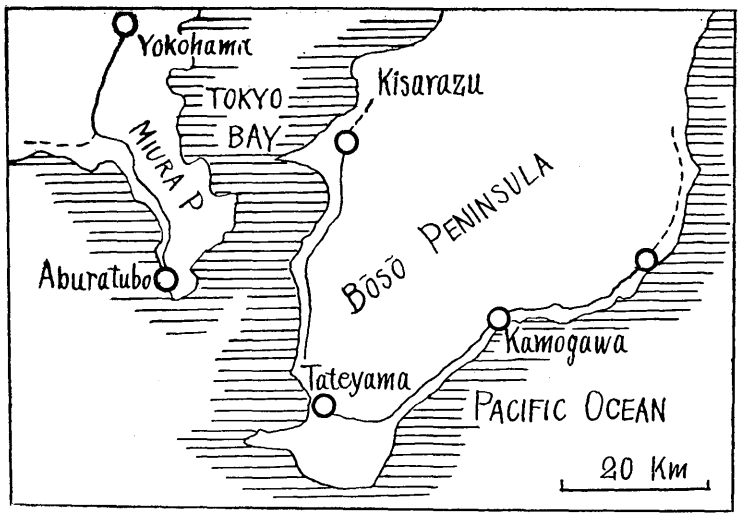

Fig. 32. Levelling route map along the coast of Bôsô Peninsula and Miura Promontory.

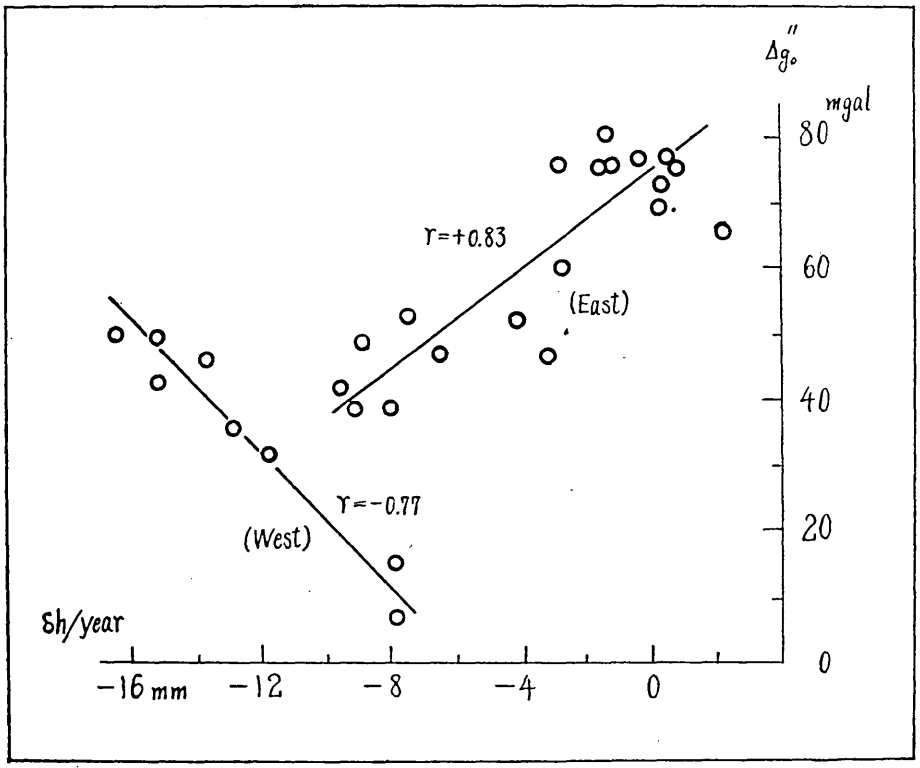

Fig. 33. Diagram of correlation between $\Delta g_0''$ and δh/year in Bôsô Peninsula.

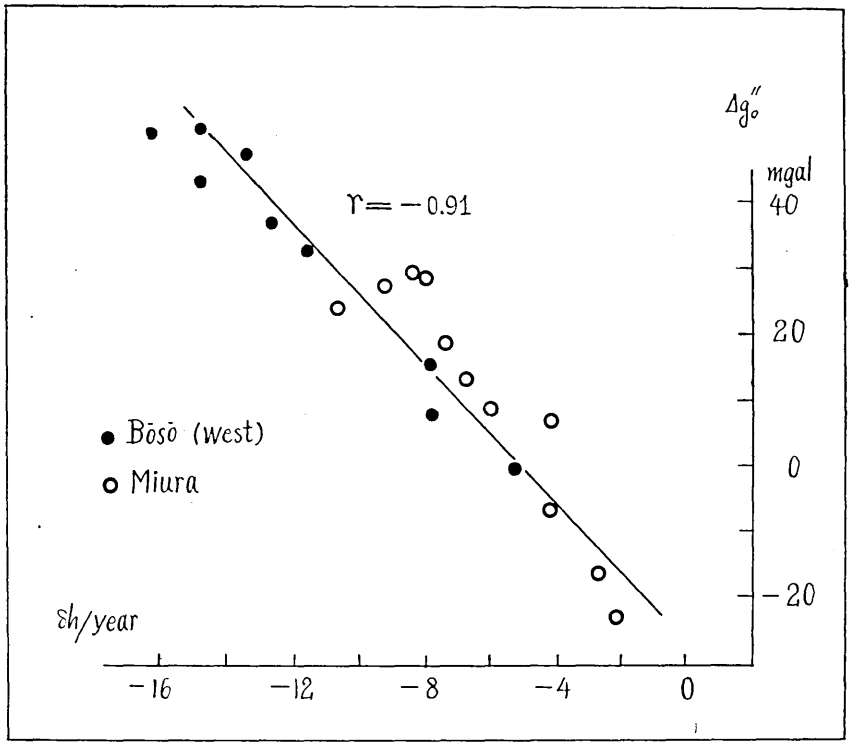

Fig. 34. Diagram of correlation between $\Delta g_0''$ and δh/year on western coast of Bôsô Peninsula and Miura Promontory.

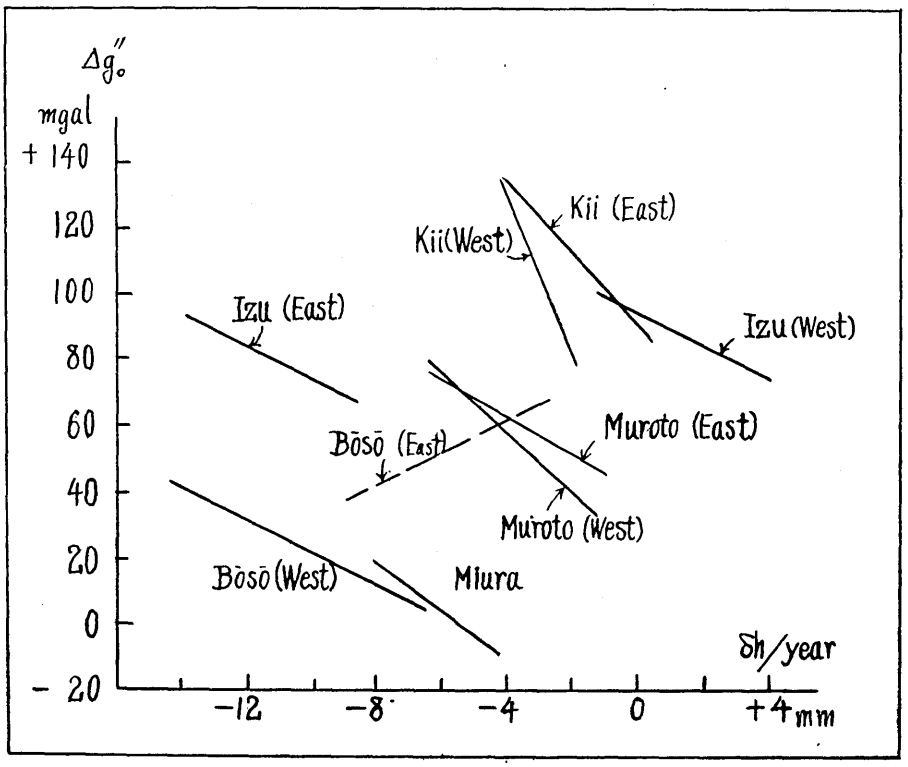

Fig. 35. Diagram of correlation between $\Delta g_0''$ and δh/year on each coastal levelling route.

All the correlation diagrams exhibit negative correlation except for the eastern coast of Bôsô peninsula. The negative regression coefficients are nearly constant for the promontories in south-western Japan including the Bôsô peninsula and there is some tendency that δh mm/year increases as $\Delta g_0''$ becomes greater. (Figs. 28–35)

§ 2. Comparison of Crustal Deformation in Japan with that in Fennoscandia

Fennoscandia is famous for crustal deformation on a large scale.[37] The deformation is thought to be the post glacial uplift as has been investigated in detail on the basis of the isostasy theory. An uplift exceeding 200 meters has been reported in the central part of Bothnia Bay since the last glacial epoch. The land is still rising at a rate of

37) W. A. HEISKANEN, F. A. VENING MEINESZ, *The Earth and Its Gravity Field* (1953), 213.

10 mm/year at its maximum along the coast of Bothnia Bay. The deformation there has been studied by adopting precise geodetic methods in Finland since 1890.

According to these studies, the amount of uplift is 900 mm/century at the Finnish coast and 1000 mm/century at the Swedish side along the northern part of Bothnia Bay getting gradually smaller as we go to the south. The zero line for the upheaval runs from the coast of Leningrad to the western coast of Norway via the southern coast of Sweden. The negative gravity anomaly increases with the increase in the uplifting movement as shown in Fig. 36.

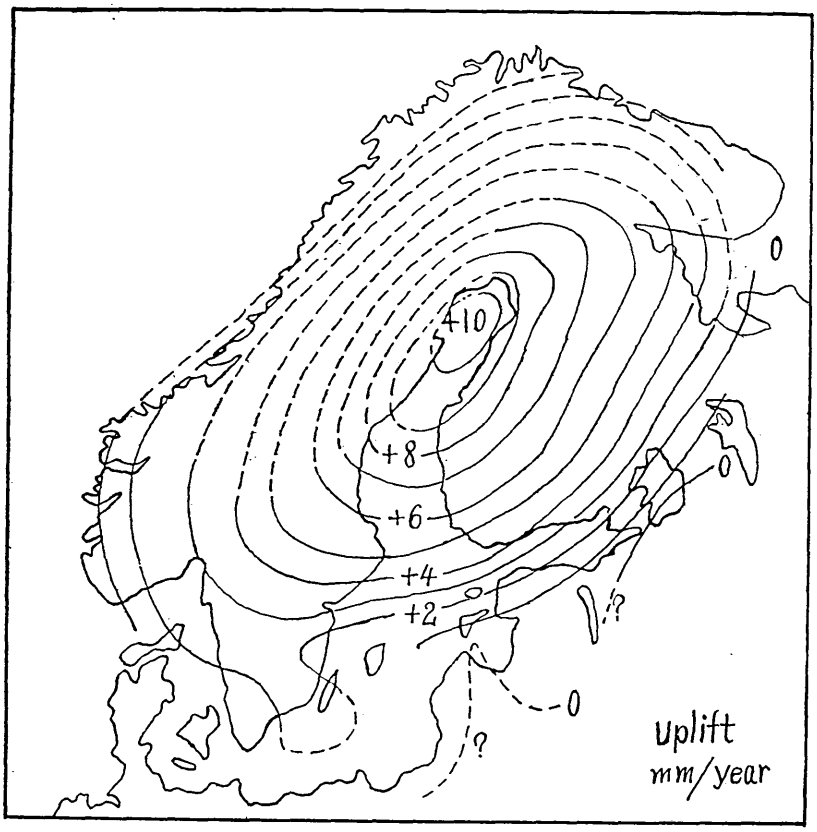

Fig. 36. Uplift in Fennoscandia (after W. A. Heiskanen and A. Kvale).

It is said that the thickness of glacier had been about 2000 meters resulting in the subsidence of the crust owing to the load of ice cap in order to keep isostatic equilibrium. On that occasion, some material of

the subcrustal layer shifted towards the environs where the load of ice cap area had been small causing a little uplift there. After the ice cap had melted away, the upheaval movement began slowly in order to attain the new equilibrium. Although the beginning of such upheaval seems likely to be at the recession stage of glaciation, the rate of upheaval is so small that it is still going on even at the present time. There is no doubt that some upheaval of the sea level owing to the melting of glacier must have taken place, but the crustal upheaval itself would be far more important in discussing the defomation in this part of the earth. Even at the present time, it is presumed that the crustal material pressed to the environs is shifting towards the interior. The explanation of the gradient of gravity anomaly, that decreases towards the interior, cannot be effected if only crustal movements taking place downwards or upwards are assumed respectively before or after the ice load, because the mass under the crust remains constant. Therefore, the only way to account for the negative gradient increasing towards the interior would be the outward shift of the subcrustal mass when the load was large.

According to Dr. Niskanen, the upheaval movement will continue for a period of 200 years or more in order to complete isostatic equilibrium, while Dr. Kvale[38] is of the opinion that the central area is too small to be readjusted, so that the upheaval would not exceed 200 meters.

In Fig. 36 is shown the distribution of the annual mean velocity δh mm/year of the upheaval in Fennoscandia. The maximum velocity of the upheaval is found somewhere in Bothnia. The correlation between δh mm/year and the gravity anomaly is studied as can be seen in Fig. 37 which clearly indicates a negative correlation.

The author would here like to compare the correlation diagrams in Fennoscandia with those in south-western Japan, (Figs. 26, 27). In Fig. 38 are plotted the Δg_i (isostatic) for Fennoscandia together with those for the Muroto and Kii districts in Japan taking δh mm/year as the abscissa. The group of points for Fennoscandia seems to overlap those for Japan around a point specified by δh mm/year $=2$–4 mm and $\Delta g_0'' = 20$ mgal.

It is interesting that this point lies on the nodal line of vertical displacement although the reason why it is so not clear. There is aseismic zone beneath the North Sea along the coast of Norway, while a highly

38) ANDERS KVALE, "Norwegian Earthquakes in Relation to Tectonics," *Arbok for Universitetet I Bergen*, No. 10, (1960).

active seismic region underlies the sea off the coast of the Japanese Island arc.

It might be said that the seismic regions correspond to those where the gravity is relatively high. Dr. Miyabe has pointed out that the larger the negative gravity anomaly is, the higher is the seismic activity in certain districts in Japan.[39),40)] From what we have been dealing with in this chapter, it cannot be entirely ignored that even the positive gravity anomaly may have something to do with the degree of seismic activity.

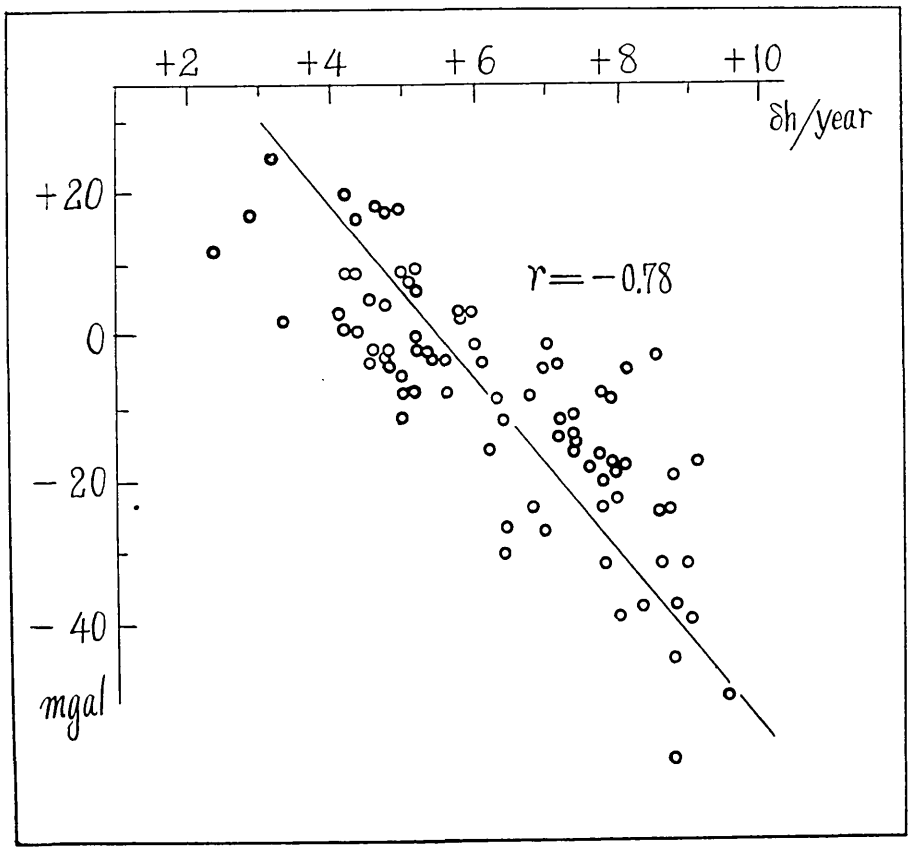

Fig. 37. Diagram of correlation between Δg_I and δh/year in Fennoscandia.

39) N. MIYABE, "Notes on Correlation between Vertical Earth Movements and Gravitational Anomalies," *Bull. Earthq. Res. Inst.*, **12** (1934), 163-173.

40) N. MIYABE, "Vertical Earth Movement in Nankai District." *Bull. Geogr. Surv. Inst.*, **4** (1955), 1-14.

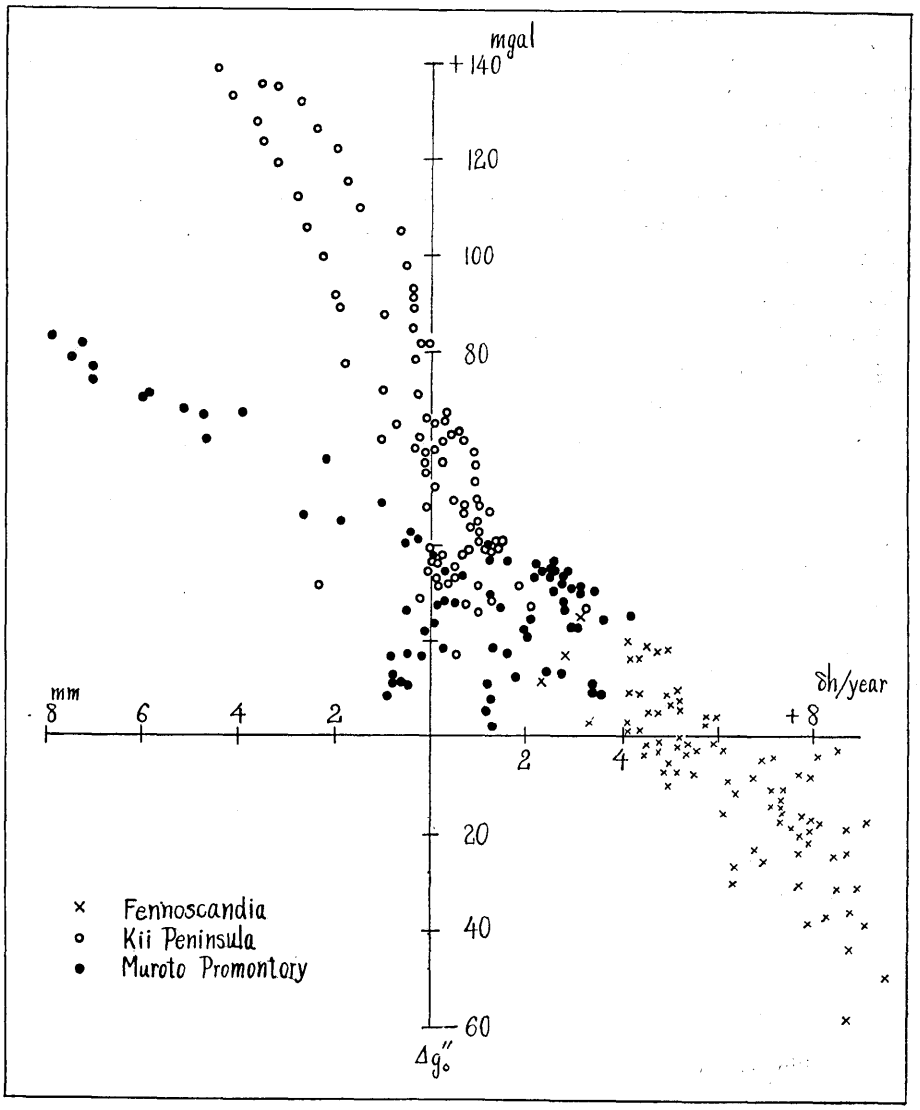

Fig. 38. Diagram of correlation between $\Delta g_0''$ (Δg_i) and δh/year in the South-western part of Japan and Fennoscandia.

§ 3. Correlation between Secular Crustal Deformation and Gravity Anomaly along the Pacific Coast-line of Japan

The relation between secular deformation and sudden upheaval accompanied by great earthquakes along the coast line of south-western

Japan has already been discussed. In this section, it is further intended to study the relation between secular crustal deformation and gravity anomaly by analysing all the available data along the levelling routes throughout Japan.[41] The influences of sudden deformation associated with earthquakes are carefully eliminated in the examination. As the fixed point of the bench marks related to the crustal deformation in Hokkaidô the datum point of Oshoro mareographical station is taken, while the one of Hosojima mareographical station and the levelling datum point of Japan (Tokyo) are taken in Kyûshû, Honshû and Shikoku Islands respectively.

Figs. 39–42 show δh mm/year and $\Delta g_0''$ for each bench mark along the Pacific coast line 4,600 km in length from Nemuro in Hokkaidô[42] to Kagosima in Kyûshû.[43] In the diagrams in Hokkaidô, there are perhaps some effects of the Tokati-oki Earthquake (Mar. 4th 1952) because no

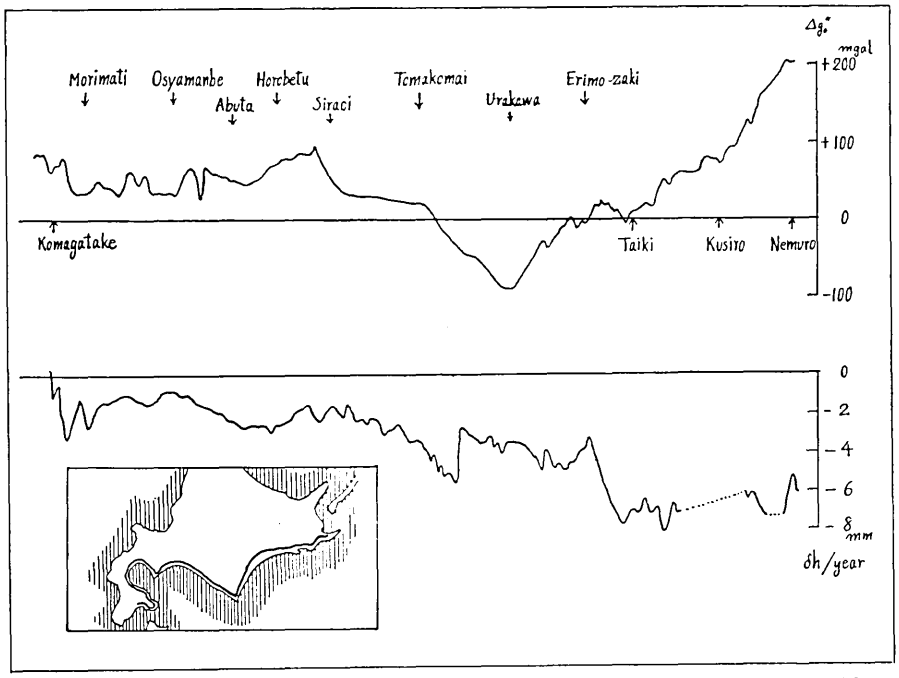

Fig. 39. Diagram of $\Delta g_0''$ and δh/year at coast-line of Pacific Ocean in Hokkaidô.

41) L. S. D. (G. S. I.), "Compilation of the 1st order precise levelling resurvey." (1930–1937).

42) G. S. I., "Gravity Survey in Japan" I. Gravity Survey in Hokkaidô District., *Bull. Geogr. Surv. Inst.*, **4** (1955), 37–99.

43) *loc. cit.*, 36).

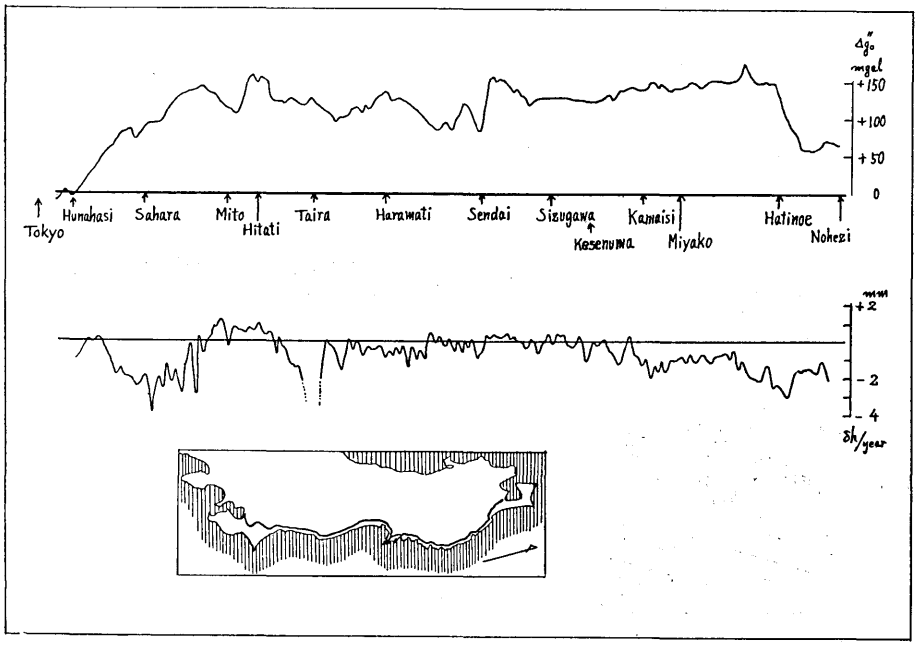

Fig. 40. Diagram of $\Delta g_0''$ and δh/year along the Sanriku coast-line in Northeastern Japan.

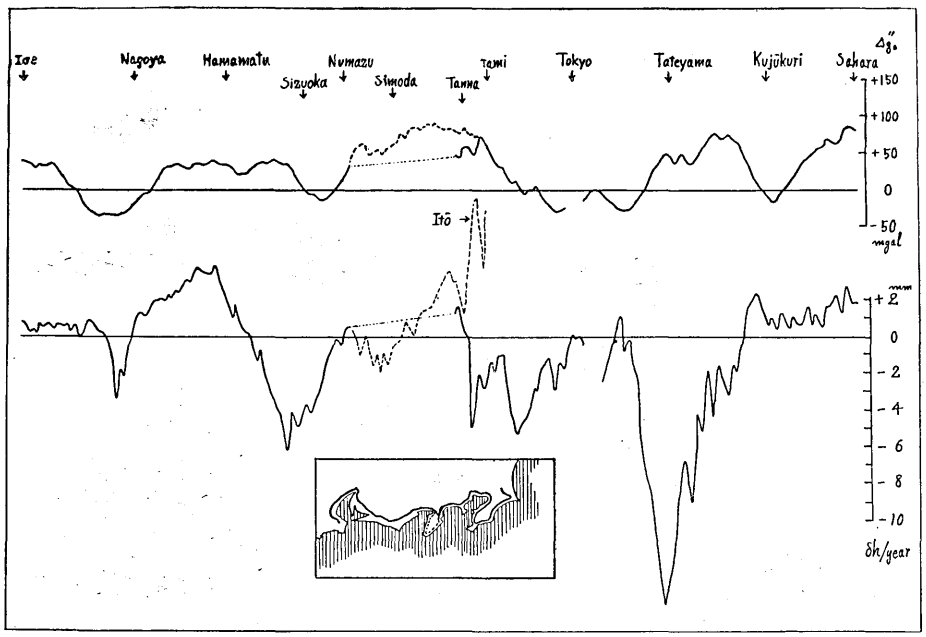

Fig. 41. Diagram of $\Delta g_0''$ and δh/year along the Tôkaidô coast-line in Central Japan.

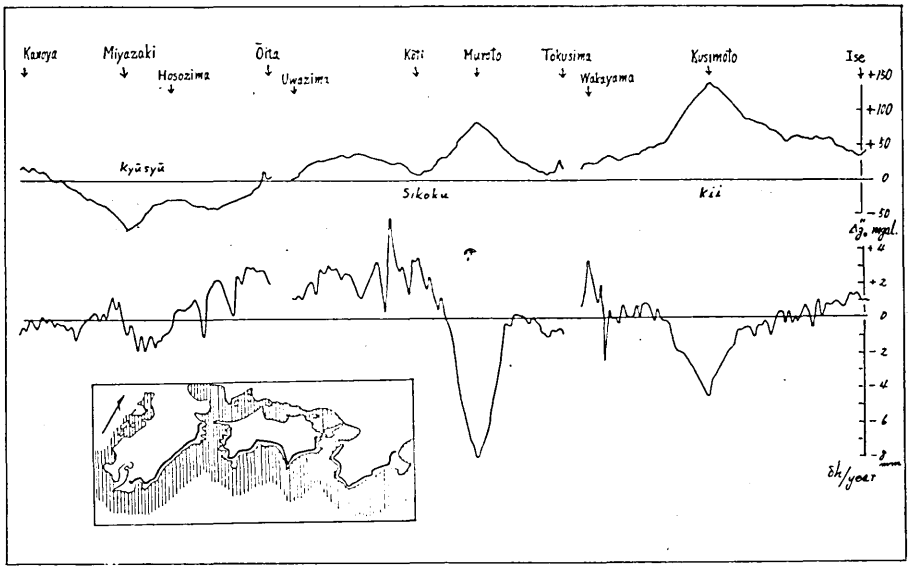

Fig. 42. Diagram of $\Delta g_0''$ and δh/year along the Nankaidô coast-line in Southwestern Japan.

Fig. 43. Correlation between $\Delta g''$ and δh/year along the coastal line of Pacific Ocean in Japan. (Continued (1)~(7))

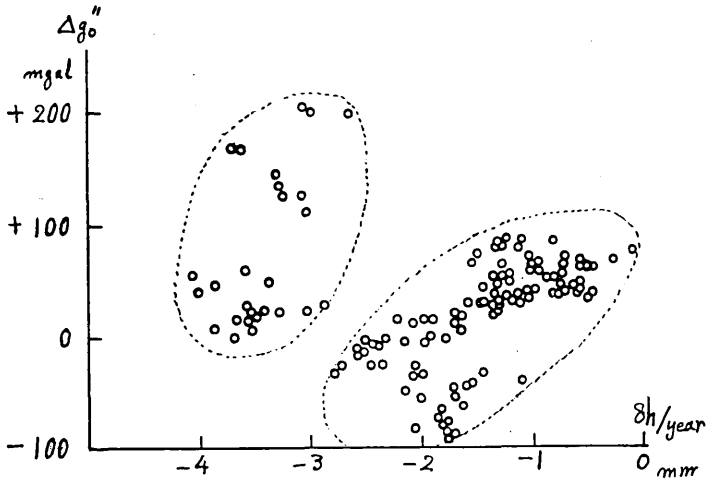

(1) Hokkaidô zone (Nemuro-Kusiro, Kusiro-Erimo-Morimati)

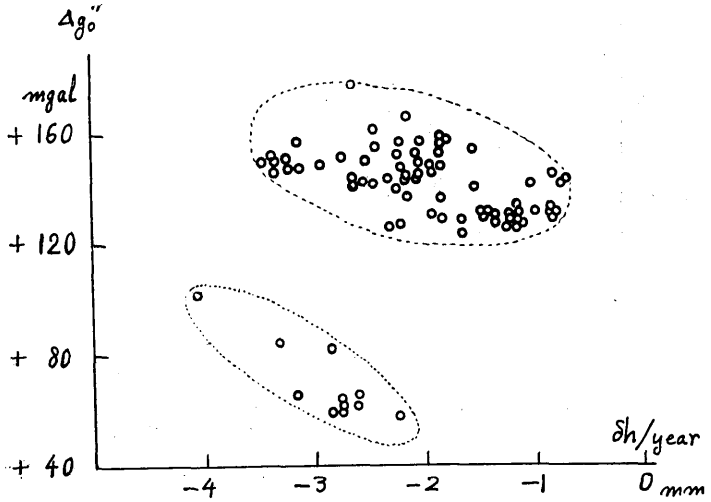

(2) Sanriku zone (Noheji-Hatinoe, Hatinoe-Kinkazan)

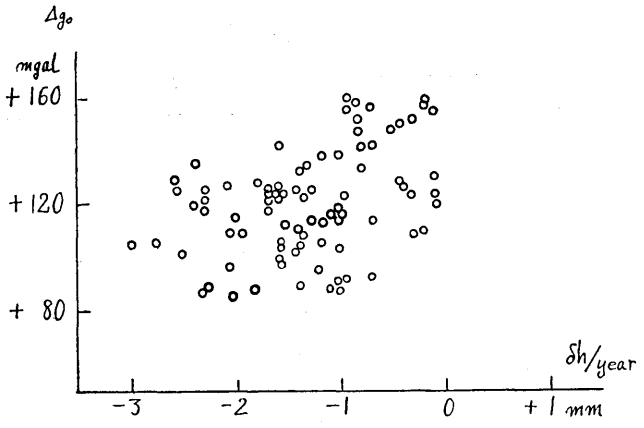

(3) Hukusima-east and Kasimanada zone (Onagawa-Sendai-Mito-Sahara)

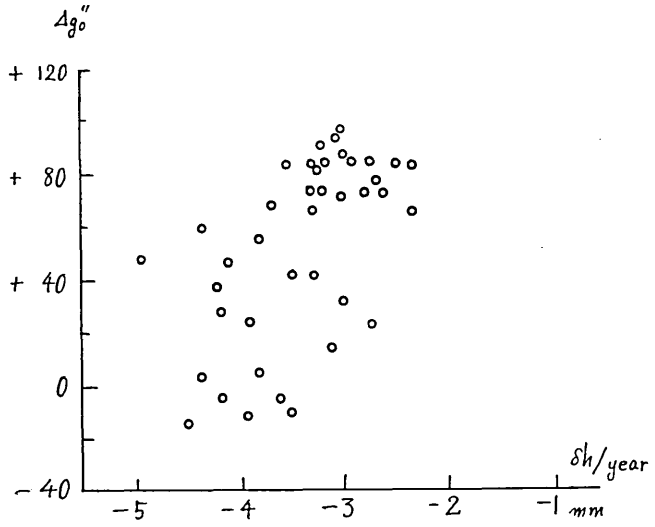

(4) Bôsô zone (Sahara-Tyôsi-Kamogawa)

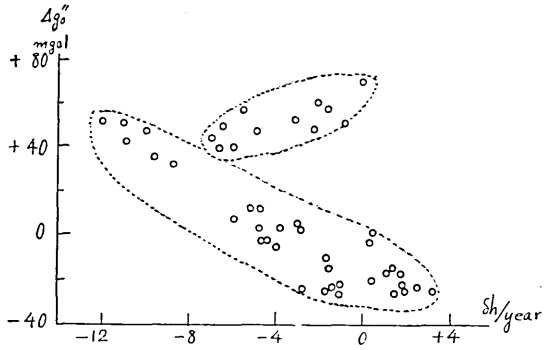

(5) Kwantô-south zone (Kamogawa-Tateyama, Tateyama-Tôkyô-Odawara)

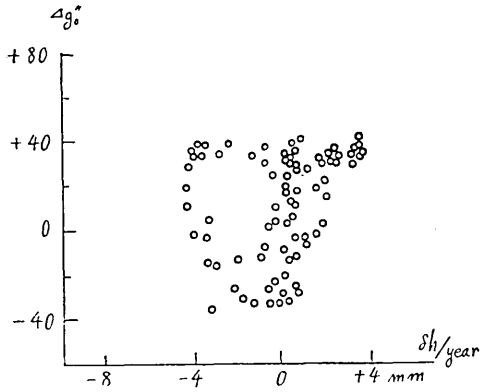

(6) Tôkaidô zone (Numazu-Nagoya-Ise)

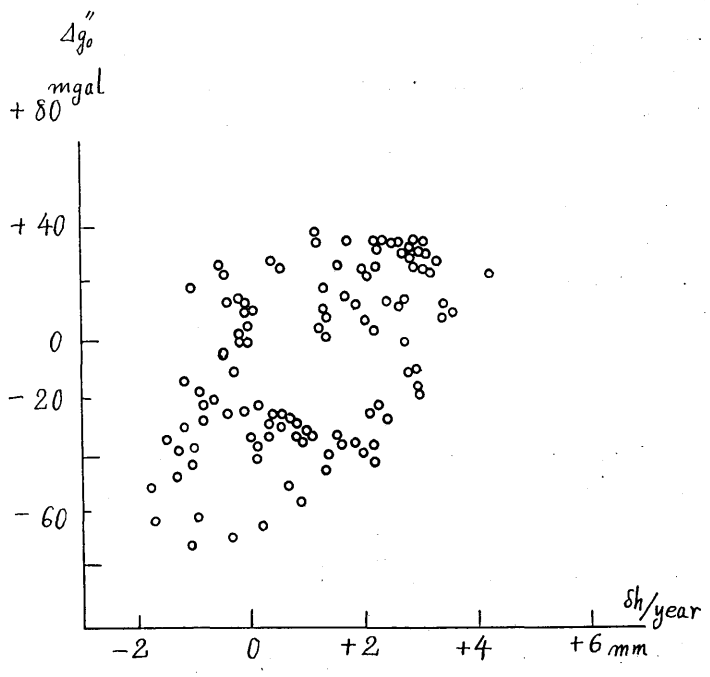

(7) Nankaidô zone (Kôti-Uwazima-Ôita-Miyazaki-Kanoya)

survey was made before it. Although a large negative anomaly is seen near Urakawa in spite of the depression of the crust on the whole, we can see positive correlation in that region. Fig. 40 shows the curves for the route from Sanriku to Tôkyô via the coast of the Kasima sea, and the deformation in this region related to higher gravity anomaly is unremarkable. The coast of the Kuzyûkuri-Bôsô-Tôkaidô-Nagoya-Ise line is shown in Fig. 41. Discussion about each peninsula or promontory has already been made. It can be said, however, that there is a predominant positive correlation on the whole. Fig. 42 shows the curve for the south-western part of Japan from the Kii peninsula to Kyûshû Island through the southern coast of Shikoku Island. In Fig. 43 (1–7), the correlation diagrams showing the relation between δh mm/year and $\Delta g_0''$ illustrate each route cited above.

1) *Southern coast line of Hokkaidô.*

The mode of correlation on the eastern side of Erimo point differs from the one on its western side. It seems likely that this difference is caused not by the effect of the Tokati-oki Earthquake but by the

difference in geological divided by the Hidaka Mountain Range.

2) *Noheji-Kinkazan.*

This region was damaged by "Tsunami" accompanying the Sanriku Earthquake (1933), and the levelling resurvey was carried out after the earthquake. But the crustal movement due to the earthquake has not been determined and the correlation seems negative over the whole region except near Hatinoe city.

3) *Onagawa-Sendai-Mito-Sahara.*

This region also shows a positive correlation. The remarkable depression observed near Taira city was caused by the excavation at Zyôban coal field, therefore this area is neglected.

4) *Sahara-Kuzyûkuri-Kamogawa.*

This region, the main part of the eastern Bôsô peninsula shows a positive correlation. The negative correlation zone in Tôkyô Bay spreading to the Kuzyûkuri coast line is similar to the negative one along the coast around the bay which is in the southern part of Japan.

5) *Kamogawa-Tateyama-Tôkyô-Odawara.*

The mode of correlation in this region is divided into two groups, one is Kamogawa-Tateyama (positive zone) and the other is Tateyama-Tôkyô-Odawara (negative). It is a very interesting phenomenon that the sign of correlation changes conspicuously at the point of the Bôsô peninsula.

6) *Numazu.Nagoya-Ise.*

As already mentioned, regarding the Izu coast line, the crustal movement is obviously disturbed by the Itô Earthquake swarm in the neighbourhood of Itô city. Atami-Numazu route crossing the Hakone Mountain Range is also disturbed by the activity of the Tanna fault.

7) *Kôti-Uwajima-Ôita-Miyazaki-Kanoya.*

There is a highly negative correlation region in Kii and Muroto as before mentioned, while the correlation is slightly negative in the west of Kôti. The coast of the Bay of Hyûga also exhibits a highly negative correlation.

The distribution of the signs of correlation is shown in Fig. 44. It may be said that great earthquakes[44] whose magnitude is greater than

44) *loc. cit.*, 21).

7.5 occur in the negative correlation zone.

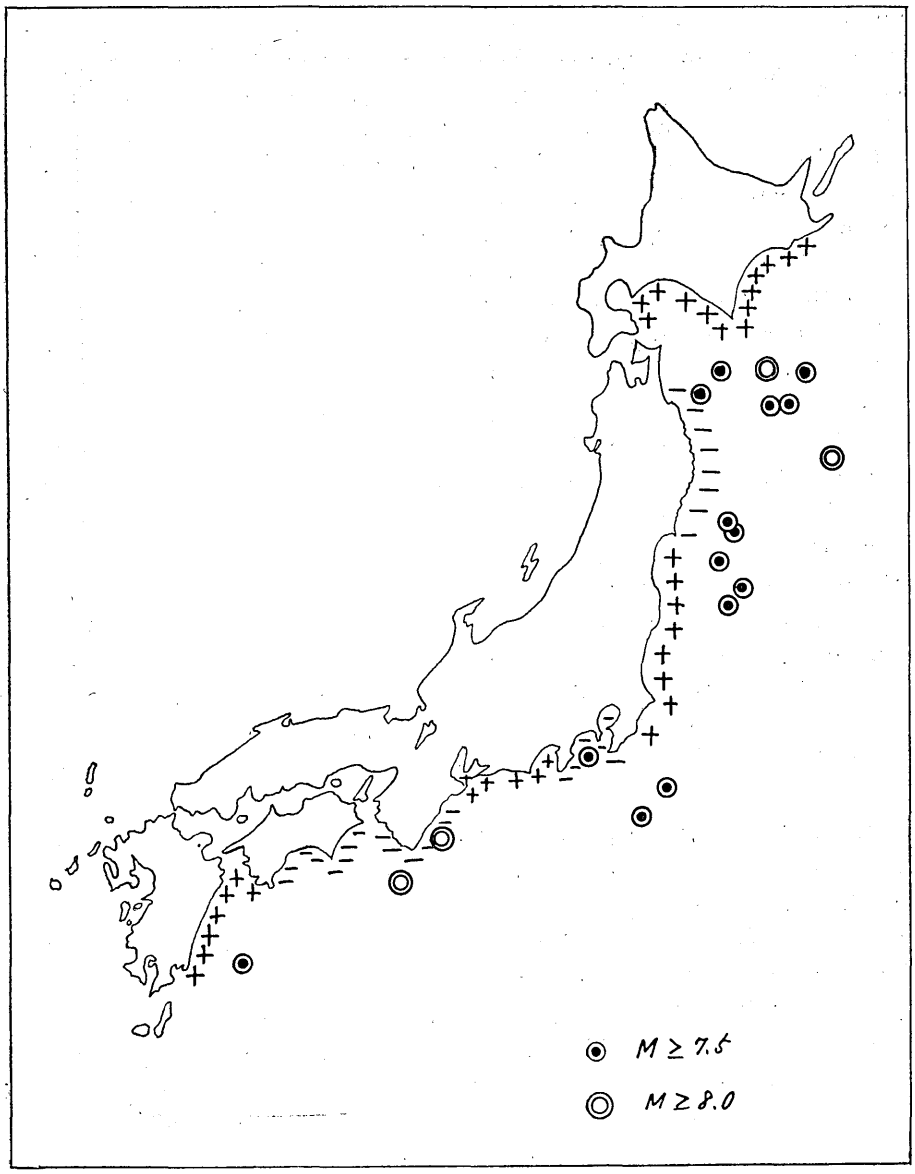

Fig. 44. The map showing distribution of the correlation (positive or negative) between $\Delta g_0''$ and δh/year in the Pacific coast-line of Japan.

Conclusion

It is hardly possible to say that precise surveys which are useful

for detecting crustal deformations are frequently carried out in foreign countries. Japan is the only country where crustal deformation is well studied by means of precise geodetic observation. The intention of this paper has been to analyse crustal deformations, some of them having been measured by the author himself, from various points of view.

(1) The conclusions of the present study may be summarized as follows. Crustal deformations are classified according to the type of distribution of vertical displacement obtained by levelling resurvey. It is emphasised that we have a particular mode of deformation in association with earthquakes which occur in and near Japan. In addition, secular deformation is also noticeable when there is no earthquake.

It seems likely that there must be some causality between sudden and secular deformations. This problem, that is closely related to the cause of great earthquakes, is the most important. It is highly desirable to conduct further studies on the relation between seismic activity and crustal deformation of this kind.

(2) Concerning local and destructive inland earthquakes, depth of earthquake origin is approximately estimated on the assumption that the crustal deformation is caused by the increase in hydrostatic pressure in an underground sphere, the earth being treated as a semi-infinite elastic medium. It is found that the depths of sphere thus estimated are shallower than the ones obtained seismometrically. Even the pressure increase supposed in the sphere can be estimated as 100–300 atm. for the earthquakes analysed.

(3) High negative correlation between the gravity anomaly and the mean velocity of the secular vertical displacement is found at the points of peninsula or promontory in the southern part of Japan. From the regression coefficient obtained for sudden and secular deformation, it is understandable that a great earthquake occurs every 100–200 years in this district. The integrated deformation due to the secular one reaches the same order as the sudden one associated with an earthquake.

Comparing the mode of secular upheaval in Fennoscandia with the secular depression in Japan, we can see a similar tendency, and their correlation diagrams suggest that the physical mechanism which causes deformations could be similar for both cases though the geological structure is different in each case.

Furthermore, it is an interesting fact that the correletion between the gravity anomaly and the secular crustal deformation in Japan is almost always negative in some areas along the Pacific coast where

many great earthquakes, larger than 7.5 in magnitude, are taking place. In other areas where we have no great earthquakes the correlation seems to be positive.

Acknowledgment

The author would like to express his sincere thanks to Prof. Yoshio Katô and Prof. Zirô Suzuki, Geophysical Institute, Tôhoku University, for the kind advice and valuable suggestions given by them.

The author is also indebted to Prof. Takesi Nagata, Geophysical Institute, Prof. Takahiro Hagiwara and Prof. Tsuneji Rikitake, Earthquake Research Institute, Tôkyô University and Dr. Sadanori Murauchi, National Science Museum, for their kindness and helpful discussion throughout the course of this study.

---

21. 地殻変動における二，三の特性

地震研究所　岡　田　　惇

地殻変動の研究は測地学の発達と共に多く行われ，とくに日本では全国に拡がる水準路線の繰り返し測量によつて水準点の垂直変動から明らかにされてきた．これらの垂直変動の内で日本列島およびその周辺に発生する大地震と急激な変動の関係，大地震の起らないときに進行する緩慢な変動と重力異常との相関等の再検討を試みた．

1. 地殻の垂直変動の分類

垂直の地殻変動を繰返し行われた精密水準測量の結果について，大地震によつて引き起された急激な変動と，大きな地震が起らない時に進行している緩慢な変動とを，夫々三つに分類することができる．大地震については地理的には日本列島において，内陸を含めて日本海側に発生するものを内陸性，太平洋沿岸に発生するものを外洋性と区分されるが，地殻変動をともなう大地震の規模は，magnitude と depth によつて異る．今までに観測された地殻の垂直変動の type は隆起型，断層型，沈降型の三つに示されるようである．水準路線が通つていないために観測できない場合も多いのであるが，前述のような三つの型の地殻変動をともなう大地震の発生する地域についての規則性ないしは周期性は明瞭でない．

Table 4. Bouguer anomaly and yearly mean of vertical displacement of bench marks.

(1) Hokkaidô

BM. No.	$\Delta g_0''$	δh/year	Loc.	BM. No.	$\Delta g_0''$	δh/year	Loc.
8354	+200.1	− 6.0	Akkesi	7989	− 28.0	− 4.7	
8353	+201.0	− 5.2		7986	− 33.7	− 4.1	Urakawa
8351	+202.0	− 5.9		7984	− 38.5	− 3.9	
7606	+169.2	− 7.3		7982	− 29.4	− 4.9	
7605	+167.6	− 7.3		7979	− 36.1	− 4.2	
7600	+145.3	− 6.6	Kusiro	7977	− 49.1	− 4.3	
7598	+135.5	− 6.5		7975	− 57.7	− 4.0	
7596	+122.0	− 6.1		7973	− 65.7	− 3.7	
7593	+126.4	− 6.4		7971	− 78.9	− 3.5	
J.43	+112.7	− 6.0		7968	− 85.8	− 3.5	
7585	+ 57.6	− 7.1		7965	− 89.1	− 3.5	
8118	+ 42.9	− 6.7		7961	− 89.3	− 3.4	
8113	+ 45.1	− 7.7		7959	− 85.4	− 4.1	
8111	+ 51.8	− 8.1		7957	− 80.2	− 3.5	
8109	+ 40.5	− 8.0		7954	− 76.4	− 3.7	
8091	+ 20.2	− 6.9		7951	− 65.7	− 3.2	
8089	+ 23.6	− 7.1		7949	− 56.3	− 3.4	Monbetsu
8087	+ 19.3	− 7.1		7823	− 49.6	− 3.4	
8085	+ 18.0	− 6.5		7822	− 47.7	− 3.2	
8083	+ 14.2	− 7.1		7821	− 45.5	− 3.1	
8081	+ 3.1	− 7.0		7819	− 41.2	− 2.1	
8077	− 3.5	− 7.4		7818	− 37.6	− 2.8	
J.34	+ 5.6	− 7.7	Taiki	7817	− 33.1	− 5.6	
8048	+ 12.3	− 7.3		7816	− 27.4	− 5.4	
8042	+ 22.5	− 6.8		7815	− 22.4	− 5.2	
8040	+ 20.3	− 6.0		7814	− 16.7	− 5.2	
8038	+ 24.8	− 5.7		7813	− 12.1	− 4.7	
8025	+ 17.6	− 3.9		7812	− 4.9	− 5.0	
8016	+ 2.6	− 3.3	Erimo	7809	+ 10.9	− 4.1	
8014	− 4.1	− 3.6		7808	+ 14.1	− 4.4	
8013	− 1.4	− 3.8		7807	+ 14.6	− 3.8	
8009	− 10.0	− 3.9		7245	+ 19.1	− 3.4	
8006	− 8.4	− 4.3		7244	+ 20.2	− 3.4	
8000	− 4.9	− 4.6		7243	+ 20.5	− 3.2	
7996	− 9.1	− 5.0		7241	+ 21.7	− 2.7	
7995	− 12.5	− 4.9		7240	+ 22.6	− 2.6	
7992	− 24.2	− 4.6		7239	+ 23.9	− 2.7	

(2) Hokkaidô

BM. No.	$\Delta g_0''$	δh/year	Loc.	BM. No.	$\Delta g_0''$	δh/year	Loc.
7238	+ 24.9	− 2.7		7168	+ 47.8	− 1.1	
7237	+ 25.7	− 2.9		7165	+ 33.8	− 0.9	
7236	+ 26.8	− 3.1	Tomakomai	6455	+ 31.8	− 0.9	
7235	+ 27.3	− 2.8		6452	+ 35.3	− 1.4	
7234	+ 27.9	− 2.3		J.20	+ 35.6	− 1.5	
7233	+ 28.1	− 2.2		5988	+ 56.2	− 1.4	
7232	+ 28.6	− 2.5		5981	+ 61.3	− 1.0	
7231	+ 29.1	− 2.3		5977	+ 35.4	− 1.2	
7230	+ 29.5	− 2.4		5976	+ 35.1	− 1.2	Morimati
7229	+ 30.1	− 2.4		5969	+ 50.8	− 1.7	
7227	+ 33.6	− 1.5		J.19	+ 37.8	− 2.7	
7226	+ 35.3	− 2.1		7062	+ 34.2	− 1.2	
7224	+ 42.9	− 1.9		7059	+ 35.4	− 1.6	
7223	+ 50.7	− 1.6		7058	+ 38.9	− 2.3	
7222	+ 58.3	− 1.8	Siraoi	7049	+ 77.8	− 3.3	
7221	+ 66.2	− 2.0		7048	+ 76.3	− 2.1	
7220	+ 78.2	− 2.4		7046	+ 69.1	− 0.5	
7218	+ 84.4	− 2.2		7045	+ 63.2	− 0.9	
7217	+ 85.2	− 1.6		7043	+ 75.6	+ 0.2	Usujiri
7214	+ 77.9	− 2.3					
7213	+ 79.3	− 2.5	Horobetu				
7212	+ 78.0	− 2.5					
7208	+ 72.4	− 2.6					
7207	+ 72.0	− 2.6					
7206	+ 70.3	− 2.9					
7203	+ 62.1	− 2.5					
7202	+ 58.7	− 2.5					
7199	+ 53.0	− 2.5					
7198	+ 48.7	− 2.6					
7197	+ 47.6	− 2.6					
7196	+ 46.7	− 2.8					
7194	+ 51.5	− 2.5					
7193	+ 53.9	− 2.4					
J. 6	+ 52.2	− 2.4	Abuta				
7192	+ 57.5	− 2.1					
7190	+ 61.0	− 1.9					
7187	+ 61.4	− 1.9					
7173	+ 67.3	− 1.4					
7171	+ 63.9	− 1.1	Osyamambe				

(3) Honsyû (Nohezi–Sizugawa)

BM. No.	$\Delta g_0''$	δh/year	Loc.	BM. No.	$\Delta g_0''$	δh/year	Loc.
6031	+ 71.0	− 3.1	Noheji	6879	+140.2	− 2.6	
6029	+ 69.4	− 2.7		6876	+147.1	− 2.9	
6026	+ 67.3	− 2.2		6875	+149.5	− 2.5	
6020	+ 58.6	− 2.8		6872	+146.5	− 3.1	Yamada
6017	+ 62.2	− 2.7		6869	+150.0	− 2.7	
6013	+ 62.7	− 2.6		6868	+145.3	− 3.2	
6011	+ 64.2	− 2.7		6861	+140.5	− 2.4	
6008	+ 63.5	− 2.6		6859	+141.2	− 2.1	
6966	+ 81.1	− 2.8		J. 3	+142.6	− 2.6	Kamaisi
6964	+ 84.9	− 3.5		6808	+144.3	− 2.1	
6962	+102.7	− 4.0		6804	+144.0	− 1.9	
6958	+144.7	− 3.3	Hatinoe	6802	+143.6	− 0.8	
6956	+149.8	− 3.4		6799	+139.8	− 1.5	
6954	+153.7	− 2.4		6794	+140.2	− 2.5	
6951	+149.7	− 3.3		6793	+135.3	− 2.1	
6950	+150.2	− 3.2		6790	+129.7	− 1.9	
6948	+149.8	− 3.2		6788	+134.0	− 1.8	
6944	+157.7	− 3.1		6787	+129.7	− 1.1	Ôhunado
6937	+176.4	− 2.6		6782	+127.7	− 1.1	
6934	+165.3	− 2.1		6779	+126.8	− 1.3	
6932	+160.0	− 2.4	Kuji	6775	+124.4	− 1.2	
6930	+152.3	− 1.5		6773	+125.1	− 2.3	
6928	+151.3	− 2.0		6771	+124.5	− 2.2	
6926	+154.5	− 1.8		6769	+128.1	− 1.1	
6924	+155.5	− 1.8		6767	+129.7	− 0.9	
6922	+156.1	− 1.8		5710	+128.9	− 1.4	
6919	+155.0	− 1.8		5708	+127.2	− 1.6	
6917	+153.4	− 2.0		5705	+128.0	− 1.4	
6909	+150.2	− 2.2		5702	+130.8	− 0.8	
6908	+148.9	− 1.9		5700	+131.7	− 0.8	
6907	+146.7	− 1.8		5698	+129.8	− 0.8	Sizugawa
6900	+149.0	− 2.2		5696	+130.8	− 1.4	
6897	+150.6	− 2.0		5693	+131.6	− 0.8	
6894	+151.9	− 1.8		5691	+129.9	− 1.2	
6891	+146.7	− 2.2		5689	+128.5	− 1.4	
6888	+144.6	− 2.0		5687	+127.2	− 1.8	
6886	+143.5	− 2.0	Miyako	5684	+126.1	− 1.2	
6884	+142.2	− 2.3		5682	+125.1	− 1.1	
6881	+139.6	− 2.2		5679	+122.5	− 1.6	

(4) Honsyû (Sizugawa–Takahagi)

BM. No.	$\Delta g_0''$	δh/year	Loc.	BM. No.	$\Delta g_0''$	δh/year	Loc.
5676	+130.8	− 1.4		5593	+132.9	− 1.4	
5675	+133.6	− 1.1		5599	+115.7	− 1.4	
5673	+140.3	− 0.7		5601	+119.3	− 1.7	
J. 2	+137.8	− 1.0	Isinomaki	5603	+115.1	− 1.3	
5629	+143.1	− 0.7		5605	+116.3	− 1.1	
5631	+148.7	− 0.8		5607	+118.3	− 1.4	
5635	+153.7	− 0.8	Ojika	5609	+117.9	− 1.0	Tomioka
5638	+155.9	− 0.9	Promontry	5611	+113.1	− 1.6	
5642	+157.2	− 0.7		5613	+101.8	− 2.5	
5644	+160.5	− 0.9		5615	+ 98.3	− 1.6	
5646	+160.3	− 0.8	Ayukawa	5617	+102.0	− 1.4	
5671	+124.2	− 1.7	Isinomaki	5619	+ 96.4	− 1.2	
5665	+ 87.7	− 1.8		5621	+104.6	− 1.0	
5663	+ 85.0	− 2.0		5623	+109.6	− 1.9	
5661	+ 95.5	− 1.0		5625	+110.8	− 4.6	
5659	+105.4	− 1.6	Matusima	5627	+116.3	− 6.2	
5656	+119.8	− 1.0		J. 4201	+116.3	− 7.4	Taira
5654	+122.9	− 1.7		4197	+126.2	− 4.4	
5651	+105.1	− 1.2		4195	+121.6	− 3.9	
5649	+ 99.6	− 1.6	Sendai	4193	+121.1	− 2.8	
2178	+ 87.1	− 1.0		4191	+123.5	− 2.3	
2176	+ 88.1	− 1.4		4189	+126.0	− 2.3	
J. 2169	+ 91.6	− 0.9	Iwanuma	4187	+127.5	− 2.1	
5561	+ 88.0	− 1.1		4185	+125.4	− 1.6	
5563	+ 92.1	− 0.7		4183	+123.7	− 1.3	
5565	+ 91.0	− 1.0		4180	+123.4	− 0.9	
5567	+ 96.5	− 2.1		4178	+124.5	− 1.6	
5569	+104.2	− 1.6		4176	+127.5	− 0.4	Takahagi
5571	+108.2	− 2.1		4174	+129.5	− 0.4	
5572	+110.5	− 1.4		4172	+149.7	− 0.5	
5574	+116.1	− 2.0		4170	+155.6	− 0.1	
5576	+120.0	− 2.4		4169	+156.0	− 0.2	
5578	+124.1	− 1.3	Nakamura	4167	+153.8	− 0.3	
5580	+125.9	− 1.7		4165	+160.8	− 0.2	
5582	+125.0	− 1.4		4163	+152.4	− 0.4	
5584	+124.4	− 1.7		4161	+123.6	− 0.3	
5586	+123.8	− 1.6		4159	+110.6	− 0.2	
5589	+129.8	− 1.8		4157	+109.0	− 0.3	
5591	+135.6	− 1.3	Haramati	4154	+114.3	− 1.2	

(5) Honshû (Takahagi–Kanaya)

BM. No.	$\Delta g_0''$	δh/year	Loc.	BM. No.	$\Delta g_0''$	δh/year	Loc.
4152	+115.6	− 0.7		3949	+ 42.4	− 3.5	
4055	+120.3	+ 0.2	Mito	3946	+ 29.6	− 4.2	
4053	+123.5	− 0.1		3944	+ 22.2	− 4.2	
4051	+130.8	− 0.1		3942	+ 12.5	− 3.9	
4049	+134.5	− 0.8		3940	+ 4.0	− 4.4	Narutô
4047	+139.2	− 1.0		3936	− 8.5	− 3.6	
4045	+143.4	− 1.6		3934	− 12.5	− 3.5	
4043	+142.0	− 0.8		3932	− 15.0	− 4.5	
4041	+139.3	− 3.9		3930	− 11.4	− 3.9	
4039	+139.1	− 1.2		3927	− 4.3	− 4.2	
4035	+136.1	− 2.4		3925	+ 4.1	− 3.8	
J. 4033	+133.7	− 3.8	Tutiura	3923	+ 12.6	− 3.1	
4031	+130.0	− 2.6		3921	+ 21.8	− 2.7	
4029	+125.7	− 2.6		3919	+ 31.6	− 3.0	
4027	+120.4	− 3.2		3917	+ 40.9	− 3.3	Ôhara
4025	+119.8	− 2.3		3915	+ 49.5	+ 2.0	
4022	+115.5	− 3.5		3911	+ 65.7	+ 1.4	
4020	+105.7	− 3.0		3909	+ 72.6	+ 0.8	
4018	+ 96.0	− 4.0		3907	+ 75.3	+ 0.6	
4017	+ 94.2	− 4.8		3905	+ 77.0	− 0.3	
4016	+ 94.9	− 3.1		3903	+ 76.1	− 1.2	
4015	+ 96.1	− 3.0		3901	+ 75.7	− 0.9	
4013	+ 91.0	− 3.2		3899	+ 77.6	+ 0.6	
J. 3981	+ 83.2	− 3.3	Sahara	3897	+ 81.1	− 0.1	
3979	+ 76.5	− 3.9		3895	+ 76.5	− 2.2	Kamogawa
3977	+ 74.1	—		3894	+ 69.5	− 0.0	
3975	+ 82.8	− 3.2		3893	+ 60.6	− 2.1	
3974	+ 85.1	—		3891	+ 52.4	− 3.1	
3973	+ 84.8	− 2.7		3889	+ 46.9	− 2.3	
3971	+ 82.9	—		3887	+ 38.9	− 6.0	
3969	+ 73.9	− 2.3		3885	+ 42.0	− 7.1	
3967	+ 69.8	− 3.7		3883	+ 47.5	− 4.9	
3966	+ 70.8	− 3.0		3881	+ 53.9	− 5.5	Tateyama
3964	+ 72.9	− 2.8		3879	+ 49.0	− 6.6	
3962	+ 73.3	− 3.2	Tyôsi	3877	+ 39.1	− 6.8	
3959	+ 63.6	− 3.3		3874	+ 46.6	−10.2	
3957	+ 61.4	− 4.4		3872	+ 50.5	−11.2	
3953	+ 50.0	− 3.8		3870	+ 50.2	−12.5	
3951	+ 46.2	− 4.1		3868	+ 42.6	−11.3	Kanaya

(6) Honsyû (Kanaya–Miura)

BM. No.	$\Delta g_0''$	δh/year	Loc.
3866	+ 36.0	− 9.6	
3863	+ 32.0	− 8.8	
3860	+ 15.0	− 6.0	
3858	+ 7.2	− 5.9	
3856	− 0.6	− 4.0	
3852	− 11.5	− 1.7	Kisarazu
3849	− 17.0	+ 0.1	
3847	− 21.4	+ 0.5	
3844	− 26.4	+ 2.0	
3841	− 26.1	+ 1.5	
3839	− 24.6	+ 3.1	
J. 3837	− 22.8	+ 2.5	Tiba
3835	− 18.1	+ 1.9	
3833	− 14.0	+ 1.3	
3829	− 0.2	+ 0.3	
J. 3827	+ 2.0	− 0.5	Hunabasi

Sahara-Sakura-Hunabasi

J. 3981	+ 83.2	− 3.3	Sahara
3983	+ 87.6	− 3.0	
3985	+ 84.3	− 2.9	
3987	+ 83.2	− 2.5	
3989	+ 79.5	− 2.7	
3991	+ 72.2	− 2.6	
3993	+ 64.7	− 2.3	Narita
3994	+ 60.4	− 2.0	
3996	+ 56.2	− 1.5	
3998	+ 48.1	− 0.9	
4000	+ 39.6	− 0.9	Sakura
4002	+ 36.1	− 1.0	
4004	+ 29.3	− 1.0	
4006	+ 21.3	− 1.3	
4008	+ 15.5	− 1.7	
4010	+ 7.3	− 1.9	
J. 3827	+ 2.0		Hunabasi

BM. No.	$\Delta g_0''$	δh/year	Loc.
29	− 23.6	+ 1.8	Kawasaki
30	− 24.8	− 1.7	
31	− 29.9	− 1.4	
32	− 27.2	− 1.9	
F.25	− 26.3	− 2.9	
34	− 23.1	− 1.1	
J. 35	− 15.9	− 1.5	
36	− 6.4	− 1.7	
J. 37	+ 6.4	− 3.0	Hujisawa
38	+ 3.3	− 2.9	
39	+ 3.3	− 3.8	
40	− 2.8	− 4.4	Hiratuka
41	− 2.8	− 4.7	
42	+ 2.8	− 4.9	
43	+ 10.1	− 5.2	
44	+ 10.1	− 4.6	
45	+ 17.4	− 4.1	
46	+ 30.2	− 1.0	
48	+ 37.3	− 1.0	
49	+ 42.6	− 1.8	
50	+ 54.2	− 1.5	
51	+ 60.4	− 2.6	
52	+ 71.0	− 2.8	Atami

Miura Promontory

J. 37	+ 6.4	− 3.0	Hujisawa
5360.1	+ 8.3	− 4.8	
5362.1	+ 12.9	− 5.6	
5363.1	+ 29.1	− 6.8	
5364.1	+ 29.1	− 7.2	
5365.1	+ 26.5	− 8.1	
5367.1	+ 23.7	− 9.4	Miura

(7) Honsyû (Atami–Hamamatu)

BM. No.	$\Delta g_0''$	δh/year	Loc.	BM. No.	$\Delta g_0''$	δh/year	Loc.
	Izu Peninsule			52.1	+ 70.6	− 2.4	Atami
				53.1	+ 63.3	− 2.1	
9328	+ 72.7	− 1.0	Atami	54	+ 54.2	− 4.9	
9331	+ 74.7	+ 2.8		55.1	+ 51.4	− 0.2	
9333	+ 77.4	+ 2.6		57.1	+ 56.5	+ 0.4	
9335	+ 77.8	− 0.3	Itô	58.1	+ 44.4	+ 1.6	
9337	+ 81.2	− 1.5		59	+ 46.1	+ 1.3	
9339	+ 79.0	− 3.5		60.1	+ 33.4	+ 0.6	Numazu
9341	+ 80.5	− 2.9		61.1	+ 19.8	+ 0.4	
9344	+ 83.4	− 1.7		62.1	+ 11.0	− 0.3	
9347	+ 86.4	− 1.7		63.1	+ 5.2	− 0.1	
9350	+ 85.7	− 1.2	Inatori	64.1	+ 0.1	− 0.3	
9352	+ 85.4	− 1.3		65.1	− 8.8	− 0.7	
9356	+ 86.2	− 1.6		66.1	− 12.1	− 1.0	
9363	+ 90.3	− 3.1		67.1	− 13.6	− 1.9	
9366	+ 88.9	− 3.1		68.1	− 13.8	− 3.0	
9368	+ 85.4	− 3.2		69.1	− 14.5	− 3.4	
9369	+ 84.6	− 3.5		70.1	− 7.2	− 4.5	
9373	+ 87.2	− 4.5		J.124	− 4.1	− 3.8	Okitu
9374	+ 86.4	− 4.6	Matuzaki	125	− 0.1	− 4.1	
9377	+ 73.4	− 4.3		126	+ 4.9	− 3.6	
9379	+ 74.2	− 4.0		127	+ 11.6	− 4.6	Shizuoka
9381	+ 79.0	− 4.6		128.1	+ 20.8	− 4.8	
9384	+ 64.5	− 5.0		129.1	+ 30.5	− 4.5	
9386	+ 64.2	− 5.1		131	+ 35.1	− 4.1	
9388	+ 62.6	− 5.7		132	+ 35.2	− 6.2	
9390	+ 54.1	− 6.2		133	+ 37.0	− 4.2	
9391	+ 51.2	− 5.7		134	+ 39.8	− 4.1	
9392	+ 54.2	− 6.6	Heta	135	+ 39.5	− 3.6	
9393	+ 53.2	− 5.7		136	+ 38.4	− 2.7	
9397	+ 50.6	− 6.3		138	+ 39.4	− 0.9	
9398	+ 52.7	− 5.7		139	+ 36.2	− 1.3	
9400	+ 64.9	− 4.7		140	+ 31.7	− 0.8	
9402	+ 61.4	− 5.5		J.141	+ 27.6	− 0.1	Kakegawa
9404	+ 58.3	− 5.7		142	+ 24.3	+ 0.2	
9406	+ 56.5	− 4.6	Numazu	143	+ 20.3	+ 0.2	
				145	+ 19.7	+ 1.6	
				146	+ 26.2	+ 1.1	
				147	+ 31.9	+ 1.8	Hamamatu

(8) Honsyû (Nagoya–Ise)

BM. No.	$\Delta g_0''$	δh/year	Loc.	BM. No.	$\Delta g_0''$	δh/year	Loc.
148	+ 33.7	+ 2.1		174.1	− 16.5	+ 0.5	Nagoya
149	+ 34.9	+ 3.1		1479	− 23.5	− 0.2	
150	+ 38.7	+ 3.7		1476	− 27.3	− 0.4	
151	+ 37.8	+ 3.8		1475	− 29.6	− 2.2	
152	+ 41.1	+ 3.5		1473	− 33.8	− 1.9	
154.1	+ 36.9	+ 3.7		1471	− 36.4	− 3.3	
155.1	+ 36.1	+ 3.8		1469	− 34.4	− 1.1	
157	+ 37.4	+ 3.7		1467	− 34.8	− 0.4	
158	+ 35.3	+ 3.5	Toyokawa	1465	− 33.6	+ 0.1	
159	+ 28.3	+ 3.0		1463	− 34.2	+ 0.3	
160	+ 30.4	+ 3.1		1461	− 33.9	0	Yokkaiti
161	+ 34.0	+ 2.7		1459	− 33.7	+ 0.6	
162	+ 35.7	+ 2.4		1457	− 32.0	+ 0.8	
163	+ 36.9	+ 2.5		1455	− 28.0	+ 0.9	
164	+ 34.3	+ 2.2	Okazaki	1453	− 20.4	+ 0.2	
165	+ 32.5	+ 2.3		1451	− 10.4	+ 0.1	
166	+ 30.4	+ 2.0		1449	− 3.6	+ 0.6	
167.1	+ 22.0	+ 2.1		1447	+ 2.8	+ 0.5	
168.1	+ 13.2	+ 2.1		J.1445	+ 5.2	+ 0.3	Tu-City
169.1	+ 3.1	+ 2.0		1484	+ 11.5	+ 0.6	
170.1	− 1.9	+ 1.6		1486	+ 17.2	+ 0.6	
171.1	− 3.9	+ 1.2		1488	+ 28.0	+ 0.7	
172.1	− 5.9	+ 1.2		1490	+ 33.5	+ 0.5	
173.1	− 14.5	+ 0.9		1492	+ 35.5	+ 0.6	
174.1	− 16.5	+ 0.5	Nagoya	1494	+ 29.6	+ 0.7	
				1496	+ 33.2	+ 0.6	
				1498	+ 34.0	+ 0.7	
				1500	+ 32.4	+ 0.3	Ise
				1502	+ 33.2	+ 0.4	
				1504	+ 35.2	+ 0.4	
				1506	+ 37.9	+ 0.6	
				1508	+ 39.8	+ 0.8	
				4737	+ 46.0	+ 1.2	
				4739	+ 39.2	+ 1.1	
				4741	+ 37.5	+ 1.2	
				4743	+ 38.8	+ 1.4	
				4745	+ 40.1	+ 1.4	
				4747	+ 40.2	+ 1.4	
				4750	+ 43.3	+ 1.0	

(9) Honsyû (Ise–Wakayama)

BM. No.	$\Delta g_0''$	δh/year	Loc.	BM. No.	$\Delta g_0''$	δh/year	Loc.
4753	+ 46.6	+ 0.7		9221	+136.9	− 4.4	Kusimoto
4755	+ 48.5	+ 1.0		9219	+131.7	− 4.1	
4756	+ 49.0	+ 1.0		9216	+127.2	− 3.7	
4759	+ 52.9	+ 0.9		9214	+121.7	− 3.5	
4761	+ 55.9	+ 0.9		9213	+117.8	− 3.2	
4762	+ 57.6	+ 0.9		9211	+110.9	− 2.8	
4764	+ 58.9	+ 0.1		9209	+105.1	− 2.6	
4766	+ 61.0	+ 1.0		9207	+ 98.4	− 2.3	
4769	+ 63.1	+ 0.6		9203	+ 90.6	− 2.0	
4771	+ 59.3	− 0.4		9201	+ 87.7	− 1.9	
4772	+ 61.4	+ 0.3		9197	+ 76.9	− 1.8	
4774	+ 61.2	+ 0.7	Owase	9191	+ 64.0	− 0.7	
4776	+ 65.0	+ 0.2		9186	+ 59.3	− 0.1	
4777	+ 65.5	− 0.1		J. 9184	+ 55.0	− 0.1	Tanabe
4779	+ 64.6	+ 0.1		4927	+ 52.1	+ 0.1	
4780	+ 63.2	− 0.2		4925	+ 48.4	+ 0.5	
4784	+ 57.4	+ 0.3		4923	+ 46.9	− 0.1	
4785	+ 55.6	− 0.1		4921	+ 45.7	+ 0.7	
4787	+ 61.6	+ 0.4		4919	+ 43.9	+ 1.0	
4791	+ 66.7	+ 0.3		4917	+ 42.7	+ 0.9	
4794	+ 70.1	− 0.3		4915	+ 38.6	+ 0.0	
4798	+ 71.4	− 1.0		4913	+ 37.7	+ 0.7	
4800	+ 77.3	− 0.3		4911	+ 36.2	+ 0.2	
4802	+ 80.8	− 0.1		4910	+ 34.1	+ 0.0	Gobô
4804	+ 80.8	− 0.2		4908	+ 31.0	+ 0.1	
4806	+ 83.6	− 0.4		4905	+ 27.5	+ 0.7	
4808	+ 85.6	− 1.0		4903	+ 28.3	− 0.3	
J. 4810	+ 87.7	− 0.4	Singu	4898	+ 31.8	+ 0.1	
4966	+ 90.3	− 0.4		4895	+ 34.7	+ 0.1	
4967	+ 92.1	− 0.4		4893	+ 33.7	+ 0.4	
4969	+ 96.9	− 0.5		4891	+ 31.2	− 2.3	
4972	+103.5	− 0.6		4889	+ 31.4	+ 1.9	
4975	+108.9	− 1.5		4887	+ 31.1	+ 1.0	
4977	+114.4	− 1.7		4885	+ 28.0	+ 1.3	
4979	+121.0	− 2.0		4883	+ 26.7	+ 2.1	
4981	+124.7	− 2.4		4881	+ 25.3	+ 3.3	
4983	+131.0	− 2.7		4877	+ 25.3	+ 1.0	
4985	+133.7	− 3.2		J. 273	+ 16.6	+ 0.6	Wakayama
4987	+134.2	− 3.5					

(10) Sikoku (Tokusima–Uwazima)

BM. No.	$\Delta g_0''$	δh/year	Loc.	BM. No.	$\Delta g_0''$	δh/year	Loc.
5074	+ 17.4	− 0.9	Tokusima	5002	+ 12.7	+ 1.8	Kôti
5077	+ 25.9	− 0.5		4995	+ 12.8	+ 2.7	
5079	+ 17.6	− 0.5		4991	+ 9.2	+ 3.5	
5081	+ 11.4	− 0.5		J. 4683	+ 9.5	+ 3.4	
5082	+ 12.0	− 0.8		4677	+ 11.3	+ 3.4	
5084	+ 8.8	− 0.9		4675	+ 19.3	+ 1.3	
5086	+ 10.2	− 0.7		4673	+ 23.1	+ 3.0	Susaki
5088	+ 12.5	− 0.8		4670	+ 23.4	+ 3.1	
5092	+ 16.8	− 0.1		4667	+ 26.1	+ 2.8	
5095	+ 18.3	+ 0.2		4664	+ 24.4	+ 3.6	
5098	+ 22.1	− 0.1		4661	+ 24.8	+ 4.2	
5102	+ 24.5	+ 0.1		4659	+ 26.4	+ 5.8	
5104	+ 27.1	+ 0.1		4657	+ 28.1	+ 0.3	Kubokawa
5106	+ 28.0	+ 0.3		4654	+ 29.6	+ 3.4	
5108	+ 33.8	+ 0.3		4652	+ 31.2	+ 3.1	
5110	+ 37.6	+ 0.1		4650	+ 31.9	+ 2.8	
5113	+ 41.4	− 0.4		4648	+ 32.9	+ 2.5	
5115	+ 40.8	− 0.3		4646	+ 33.2	+ 2.2	
5123	+ 48.2	− 1.0		4644	+ 36.3	+ 1.6	
5128	+ 57.0	− 2.2		4642	+ 37.0	+ 1.2	
5131	+ 66.5	− 4.0		4640	+ 38.8	+ 1.2	
5133	+ 65.7	− 4.8		4638	+ 34.9	+ 2.2	
5135	+ 69.8	− 6.0		4636	+ 34.8	+ 2.5	
5137	+ 73.4	− 7.1		4635	+ 34.4	+ 2.6	
5138	+ 78.0	− 7.5		4633	+ 36.0	+ 2.6	
5142	+ 82.5	− 7.9	Muroto	4631	+ 34.1	+ 2.3	Nakamura
5144	+ 79.9	− 7.3		4630	+ 34.1	+ 2.9	
5146	+ 76.2	− 7.1		4629	+ 32.9	+ 2.8	
5148	+ 70.4	− 5.9		4627	+ 30.5	+ 3.1	
5150	+ 66.9	− 5.2		4625	+ 31.3	+ 2.9	
5152	+ 61.4	− 4.7		4623	+ 30.0	+ 2.6	
5158	+ 45.5	− 2.7		4621	+ 28.5	+ 2.8	
5160	+ 44.5	− 1.9		4619	+ 27.0	+ 1.5	Sukumo
5162	+ 40.3	− 0.6		4616	+ 24.5	+ 2.1	
5164	+ 31.1	+ 0.2	Aki	4613	+ 21.2	+ 2.0	
5166	+ 33.5	+ 0.6		4608	+ 17.0	+ 1.6	
5168	+ 28.8	+ 1.3		4598	+ 10.8	+ 1.2	
5172	+ 26.6	+ 0.5		4595	+ 8.3	+ 1.3	
5174	+ 22.7	+ 2.0		4592	+ 5.2	+ 1.2	
5178	+ 13.5	+ 2.4		4590	+ 2.1	+ 1.3	Uwazima

(11) Kyûsyû (Ôita–Kanoya)

BM. No.	$\Delta g_0''$	δh/year	Loc.	BM. No.	$\Delta g_0''$	δh/year	Loc.
J 2633	—	—	Ôita	2738	− 63.9	− 1.8	
2632	+ 6.1	+ 2.0		2742	− 68.1	− 0.3	
2631	+ 4.5	+ 2.1		2744	− 71.8	− 1.0	
2627	+ 13.3	+ 2.7		2746	− 65.2	+ 0.2	
2624	− 0.2	+ 2.8		2748	− 56.9	+ 0.9	
2619	− 11.3	+ 2.9		J. 2751.1	− 50.2	+ 0.6	Miyazaki
2615	− 19.3	+ 3.0		9182	− 47.2	+ 1.3	
2613	− 20.3	+ 3.0		9179	− 40.8	+ 0.2	
2610	− 24.3	+ 2.5		9176	− 37.3	+ 0.2	
2609	− 26.4	+ 2.1		9174	− 34.9	+ 0.3	
2607	− 28.5	+ 2.5	Nobeoka	9171	− 33.7	0.0	
2605	− 31.4	+ 0.3		9169	− 30.3	+ 0.4	Hokugô
2604	− 32.3	+ 0.9		9164	− 24.7	+ 0.1	
2600	− 33.6	+ 1.5		9159	− 26.5	− 0.1	
2598	− 37.0	+ 1.9		9157	− 21.7	− 0.6	
2596	− 37.5	+ 2.2		9154	− 18.6	− 0.9	
2594	− 42.6	+ 2.2		9151	− 14.2	− 1.2	
2592	− 39.4	+ 2.0		9149	− 11.0	− 0.4	
2590	− 37.5	+ 1.6		9147	− 7.5	− 0.6	
2588	− 39.9	+ 1.4		9145	− 4.6	—	
2586	− 36.5	− 1.0		9143	− 2.8	− 0.2	
2584	− 35.8	+ 0.8		9141	− 0.9	− 0.2	
2582	− 33.8	+ 1.1		9139	1.7	− 0.3	
J. 2635	− 32.3	+ 0.9		9137	5.6	− 0.1	
2709	− 30.6	+ 0.8		9135	10.1	− 0.1	Sibusi
2712	− 38.1	+ 0.6		9133	11.1	+ 0.1	
2714	− 27.0	+ 0.6		9131	9.7	− 0.3	
2716	− 25.3	+ 0.5		9130	12.8	− 0.5	
2718	− 25.0	+ 0.4	Hosozima	9128	13.6	− 0.3	
2720	− 25.3	− 0.4		9126	12.4	− 0.1	
2722	− 26.0	− 0.8		9124	15.4	− 0.6	
2724	− 29.5	− 0.8		9122	21.5	− 0.5	
2726	− 30.0	− 1.2		9120	19.8	− 1.0	Kanoya
2728	− 31.8	− 1.2					
2730	− 36.1	− 1.6					
2732	− 43.1	− 1.0					
2734	− 48.5	− 1.4					
J. 2736	− 52.7	− 1.8					
2737	− 61.1	− 0.9					

2. 内陸性の浅発地震と隆起変動

内陸性の破壊的地震にともなつて断層は発見されなかつたが，震央附近で隆起のみが水準点の垂直変動から見出された 5 箇の地震をえらび，これらの地震によつて生じた隆起変動の地表における変形を dome up 型と仮定する．ここで半無限弾性体内における球核の圧力増加による表面変形の理論的な変形曲線に合わせることによつて，箇々の地震の仮定した球核の深さは求められる．その結果夫々の深さは非常に浅くなり，地表の弾性変形にしたがはない部分の厚さを考慮しても地震計測的な深さにはおよばない．

また一方このような変形を地表に生ぜしめるために必要な内部球核の圧力増加量は 100～300 気圧あれば説明ができる．

3. 緩漫な変動と重力異常の相関

本州西南太平洋岸に沿う半島部における永年的な地殻変動の年平均速度と重力異常の相関は，房総半島東部を除いてほとんど同じ傾向で negative となつた．

同様に Fennoscandia の上昇運動と重力異常についても negative であることはよく知られているが，日本の西南太平洋岸とあわせ考えると全く両者（年平均速度と重力異常）の相関関係は良く一致していることが注目された．

さらに本州北海道東端より九州南端に至る約 4600 粁におよぶ太平洋岸の緩漫な地殻変動の年平均速度と重力異常の相関分布は，やや positive または無相関の region と明瞭に negative の region に分けることができる．また外洋性の大地震で magnitude 7.5 以上のものは後者の region に発生していることが認められる．